

**FACULTY
OF MATHEMATICS
AND PHYSICS**
Charles University

BACHELOR THESIS

Kamil Belán

**Simulating flows past a mountain range
using smoothed particle hydrodynamics**

Mathematical Institute of Charles University

Supervisor of the bachelor thesis: doc. RNDr. Michal Pavelka, Ph.D.

Study programme: Physics (B0533A110001)

Study branch: FP (0533RA110001)

Prague 2024

I declare that I carried out this bachelor thesis independently, and only with the cited sources, literature and other professional sources. It has not been used to obtain another or the same degree.

I understand that my work relates to the rights and obligations under the Act No. 121/2000 Sb., the Copyright Act, as amended, in particular the fact that the Charles University has the right to conclude a license agreement on the use of this work as a school work pursuant to Section 60 subsection 1 of the Copyright Act.

In date

Author's signature

The author would like to thank doc. Pavelka for his patient guidance and inspiring approach to science, as well as to all the consultants: Dr. Šácha, Dr. Kincl and Dominika Hájková, who devoted their time to discussing topics that must have seemed elementary to them, but never gave any indication that this was the case.

Title: Simulating flows past a mountain range using smoothed particle hydrodynamics

Author: Kamil Belán

Institute: Mathematical Institute of Charles University

Supervisor: doc. RNDr. Michal Pavelka, Ph.D., Mathematical Institute of Charles University

Abstract: The method of Smoothed Particle Hydrodynamics is applied to the phenomenon of mountain waves - atmospheric internal gravity waves generated by flows over topography. General aspects of the method and the alternative derivations of the theory using Hamiltonian continuum mechanics are discussed. The basic explanation of the physical mechanisms that generate the internal gravity waves and the review of the current state of the numerical simulation of the matter are provided. A code in the Julia programming language is written to simulate the phenomenon of mountain waves using the symplecticity of the SPH equations by utilizing a symplectic integrator. The results obtained are compared to those from the literature, and the applicability of the SPH method in meteorology is also discussed.

Keywords: smoothed particle hydrodynamics meteorology internal gravity waves

Contents

Introduction	2
1 The SPH method	3
1.1 Introduction	3
1.1.1 Strategy of smoothed particle hydrodynamics	3
1.2 Classical approach to SPH	4
1.2.1 Continuous interpolation	4
1.2.2 Discrete interpolation	6
1.3 Discrete version of fluid equations	10
1.3.1 Discrete continuity equation	10
1.3.2 Discrete Euler equations	10
1.3.3 The complete WCSPH scheme	11
1.4 SPH equations as a Hamiltonian system	12
1.4.1 Lagrange and Euler picture	13
1.4.2 Choice of the manifold	13
1.4.3 Canonical Poisson bracket in the Lagrangian frame	13
1.4.4 The SPH Poisson bracket	15
1.4.5 Hamilton equations induced by the SPH Poisson bracket	17
1.5 Summary of the SPH method	23
2 Mountain-Wave Simulations in general	24
2.1 Introduction	24
2.1.1 Current status of mountain-wave simulations	24
2.2 An introduction to the theory of internal gravity waves	25
2.2.1 Density and pressure stratification of the atmosphere	25
2.2.2 Buoyancy oscillations	27
3 Mountain-Wave Simulations using the SPH Method	30
3.1 Parameters of the simulation	30
3.1.1 Computational domain and mountain profile	30
3.1.2 Initial and boundary conditions	31
4 Results of the simulation	34
4.1 Challenges	34
4.1.1 Hydrostatic balance	35
4.1.2 Further procedure after unsatisfactory attempts to stabilize the hydrostatic balance	38
4.1.3 Boundary conditions	38
4.1.4 Sound waves	40
4.2 Results	42
Conclusion	47
Bibliography	49

Introduction

This thesis serves as an attempt to combine:

- the method of Smoothed Particle Hydrodynamics (SPH)
- the phenomenon of mountain waves, i.e., atmospheric internal gravity waves generated by a flow over topography
- numerical simulations with the use of symplectic integrators,

to provide possibly new results in the field of atmospheric dynamics, as, to the best knowledge of the author, the SPH method has not been used in this particular context before. The ultimate goal of this thesis is to be able to perform a numerical simulation within a controlled setting that would allow easy discussion of the results and the applicability of the method in meteorology.

The text is divided into four logical chapters:

- Chapter 1 summarizes the foundations of Smoothed Particle Hydrodynamics
- Chapter 2 provides a very brief insight into the theory of atmospheric internal gravity waves
- Chapter 3 connects the two previous chapters and explains some of the aspect of the SPH method in meteorological applications
- Chapter 4 discusses the results obtained by numerical simulations

1. The SPH method

1.1 Introduction

Smoothed Particle Hydrodynamics, SPH for short, is now the most popular particle method used in the scientific literature Violeau [2012]. Unlike grid methods (mesh methods), such as the finite element method, particle methods are typically easier to implement and offer a broader range of possible applications. Originally, the authors of SPH, R.A. Gingold and J.J. Monaghan, used it to solve astrophysical problems in which a considerable number of grid points ought to be used; instead, they modeled the continuum as a set of particles, each possessing a set of physical quantities (mass, momentum, energy, entropy) Gingold and Monaghan [1977], Liu [2009]. In later years, the usage of the SPH method in modeling incompressible and compressible flows has been developed. One of the main benefits of the SPH method is its consistency with the formalism of Lagrangian and Hamiltonian mechanics. We will examine this in more detail in Section 1.4. This consequently implies that the SPH equations represent a Hamiltonian system, and when the proper treatment of density is used, the system becomes symplectic Kincl and Pavelka [2023]. Symplectic systems are preferable, as they allow for symplectic integrators.

In the following sections, we present the foundation of the SPH method.

1.1.1 Strategy of smoothed particle hydrodynamics

Problems in hydrodynamics are usually formulated in the language of PDE's for some field variables (velocity, pressure, momentum, etc.) that ought to be solved in some domain with boundary conditions. The standard technique for solving such a system starts by discretizing the problem domain and then approximating the field functions (and their derivatives). The procedure produces a set of ODE's for the approximated functions with respect to time. The strategy of the SPH method follows this outline in the form Liu [2009]:

- represent the domain of the problem as a set of particles, i.e. represent the continuum as a set of discrete particles
- develop continuous integral approximation, so-called continuous interpolation, to simplify field functions
- even more simplify the interpolation using a different, discrete interpolation (summing over the “particles” of the fluid instead of integrating over the continuum)
- rewriting the governing PDE's, i.e. the continuity equation and Euler equations, using the approximations and solving them for the approximated functions

In the upcoming chapter, we follow these steps and obtain the discussed system of ODE's; for the purpose of this text, we refer to this approach as the classical approach. Later on, we derive the same set of equations exploiting the Hamiltonianity of the system.

1.2 Classical approach to SPH

1.2.1 Continuous interpolation

Assume that the fluid occupies a set $\Omega \subset \mathbb{R}^n$. An arbitrary scalar field $\Phi(t, \mathbf{x})$ describing a certain quantity of the fluid (e.g. density) can be expressed as a spatial convolution with the δ distribution

$$\Phi(t, \mathbf{x}) = (\Phi \star \delta)(t, \mathbf{x}) = \int_{\Omega} \Phi(t, \mathbf{x}') \delta(\mathbf{x} - \mathbf{x}') d\mathbf{x}' \quad (1.1)$$

The idea of interpolation originates from this identity¹, as one wishes to replace the δ distribution with a more regular function, called the interpolation kernel and denoted by $w(\mathbf{x})$. For a fixed kernel, we define the continuous interpolation of the field $\Phi(t, \mathbf{x})$ as

$$[\Phi]_w^C(t, \mathbf{x}) := \int_{\Omega} \Phi(t, \mathbf{x}') w(\mathbf{x} - \mathbf{x}') d\mathbf{x}' = (\Phi \star w)(t, \mathbf{x}) \quad (1.2)$$

The immediate question is under what conditions (what qualities should the field $\Phi(t, \mathbf{x})$ or the interpolation kernel $w(\mathbf{x})$ have?) is the interpolated field $[\Phi]_w^C(t, \mathbf{x})$ a good approximation of the field $\Phi(t, \mathbf{x})$.

Let us first consider some candidates for the interpolation kernel $w(\mathbf{x})$. It is natural to require $w(\mathbf{x})$ to have a compact support, that is, $\text{supp } w \subset B_h \subset \Omega$, where $h \in \mathbb{R}^+$ is the smallest radius of a ball B_h such that the support is contained in the ball. The δ distribution possesses this property, and, by the nature of interpolation, we are not interested in regions far away from the desired point in space. Monaghan and his use of B-splines present this approach; see Monaghan [1985]. Another possibility is to require a sufficiently fast decrease of the kernel for $\|\mathbf{x}\| \gg 1$, take, for example, the function $\exp(-\|\mathbf{x}\|^2)$. Naturally, functions such as $\exp(-\|\mathbf{x}\|^2) \chi_{[-h, h]}(\|\mathbf{x}\|)$ can be constructed combining both the requirements for sufficient decrease and a compact support.

It can be shown via Taylor expansion (see Violeau [2012]) that for an interpolation kernel $w(\mathbf{x})$ with a compact support $\text{supp } w \subset B_h \subset \Omega$ and a sufficiently smooth field $\Phi(t, \mathbf{x})$ ² that

$$[\Phi]_w^C(t, \mathbf{x}) = \Phi(t, \mathbf{x}) + \mathcal{O}(h^2), \quad (1.3)$$

if conditions

$$\int_{\Omega} w(\mathbf{x}') d\mathbf{x}' = 1, \quad (1.4)$$

$$\int_{\Omega} \mathbf{x}' w(\mathbf{x}') d\mathbf{x}' = 0 \quad (1.5)$$

hold. Condition (1.4) represents a normalisation condition, which can be easily met by scaling the kernel, that is, $w(\mathbf{x}) \equiv N \tilde{w}(\mathbf{x})$, $N = 1 / \int \tilde{w} d\mathbf{x}$. The second condition (1.5) can be met by the kernel being spherically symmetric, i.e. $w(\mathbf{x}) \equiv$

¹The identity holds for Φ being at minimum $\Phi \in L_{loc}^1(\Omega)$. As usual in the case of regular distributions, we identify the distribution with its representing function.

²For the Taylor expansion to be valid, we require the function $\mathbf{x} \mapsto \Phi(t, \mathbf{x})$, $\forall t \in \mathbb{R}^+$ to be $C^2(\Omega)$.

$w(\|\mathbf{x}\|)$ and the region Ω being invariant under central symmetry centered at the origin. In what follows, we will suppose the conditions always hold.

Continuous interpolation of differential operators

In this section, $\Phi(t, \mathbf{x})$ denotes an arbitrary scalar field and $\mathbf{F}(t, \mathbf{x})$ denotes an arbitrary vector field, both being sufficiently smooth (again, $C^2(\Omega)$ for the spatial derivatives). Our next goal is to interpolate the scalar field $\nabla \cdot \mathbf{F}(t, \mathbf{x})$ and the vector field $\nabla \Phi(t, \mathbf{x})$ ³. Let us start with the gradient of a scalar field; deploying the interpolation to the field $\nabla \Phi(t, \mathbf{x})$ yields the following.

$$[\nabla \Phi(t, \mathbf{x})]_w^C = \int_{\Omega} \nabla' \Phi(t, \mathbf{x}') w(\mathbf{x} - \mathbf{x}') d\mathbf{x}' = \int_{\Omega} \nabla' [\Phi(t, \mathbf{x}') w(\mathbf{x} - \mathbf{x}')] d\mathbf{x}' - \int_{\Omega} \Phi(t, \mathbf{x}') \nabla' w(\mathbf{x} - \mathbf{x}') d\mathbf{x}', \quad (1.6)$$

where ∇' stands for differentiation with respect to the dashed coordinates, i.e. $\nabla' = \mathbf{e}_k \frac{\partial}{\partial x'^k}$ ⁴. Using the identity Gurtin and Drugan [1984] $\nabla \Psi = \nabla \cdot (\Psi \mathbb{I})$, where \mathbb{I} is the identity tensor of order n and the Gauss theorem, we can rewrite the first integral:

$$\int_{\Omega} \nabla' [\Phi(t, \mathbf{x}') w(\mathbf{x} - \mathbf{x}')] d\mathbf{x}' = \int_{\partial\Omega} \Phi(t, \mathbf{x}') w(\mathbf{x} - \mathbf{x}') d\mathbf{S}(\mathbf{x}'),$$

where $d\mathbf{S}(\mathbf{x}') = dS \mathbf{n}(\mathbf{x}')$ stands for the $(n-1)$ hypersurface element oriented in the direction of an exterior normal vector $\mathbf{n}(\mathbf{x}')$ to the region Ω at the point $\mathbf{x}' \in \Omega$. The second integral can be rewritten using the trivial fact

$$\nabla' w(\mathbf{x} - \mathbf{x}') = -\nabla w(\mathbf{x} - \mathbf{x}') \quad (1.7)$$

These identities allow us to write

$$[\nabla \Phi(t, \mathbf{x})]_w^C = \int_{\partial\Omega} \Phi(t, \mathbf{x}') w(\mathbf{x} - \mathbf{x}') d\mathbf{S}(\mathbf{x}') + \int_{\Omega} \Phi(t, \mathbf{x}') \nabla w(\mathbf{x} - \mathbf{x}') d\mathbf{x}'$$

Supposing that $\text{dist}(\text{supp } w, \partial\Omega) \gg 1$ for a kernel w with compact support or $|\mathbf{x} - \mathbf{x}'| \gg 1, \mathbf{x} \in \Omega, \mathbf{x}' \in \partial\Omega$ for a kernel with non-compact support causes the surface integral to vanish, which finally leads to

$$[\nabla \Phi]_w^C(t, \mathbf{x}) = \int_{\Omega} \Phi(t, \mathbf{x}') \nabla w(\mathbf{x} - \mathbf{x}') d\mathbf{x}' \quad (1.8)$$

Deploying the estimate 1.3 (which remains valid also for a vector field, see Violeau [2012]) under conditions similar to those 1.4 - 1.5, we obtain the following.

$$[\nabla \Phi(t, \mathbf{x})]_w^C = \nabla \Phi(t, \mathbf{x}) + \mathcal{O}(h^2), \quad (1.9)$$

where h has the same meaning as in the previous section.

³In the previous section, only the interpolation of a scalar field has been discussed. The matter is the same for vector fields; we define $[\mathbf{F}(t, \mathbf{x})]_w := (\mathbf{F} \star w)(t, \mathbf{x})$

⁴Einstein's summation convention is used. Here, \mathbf{e}_k denote basis vectors and x'^k denote (possibly curvilinear) coordinates

In the case of the divergence of a vector field, we write

$$\begin{aligned} [\nabla \cdot \mathbf{F}]_w^C(t, \mathbf{x}) &= \int_{\Omega} \nabla' \cdot \mathbf{F}(t, \mathbf{x}') w(\mathbf{x} - \mathbf{x}') d\mathbf{x}' \\ &= \int_{\Omega} \nabla' \cdot [\mathbf{F}(t, \mathbf{x}') w(\mathbf{x} - \mathbf{x}')] d\mathbf{x}' - \int_{\Omega} \mathbf{F}(t, \mathbf{x}') \cdot \nabla' w(\mathbf{x} - \mathbf{x}') d\mathbf{x}' \end{aligned} \quad (1.10)$$

Using the same reasoning as in the case of 1.6, the first integral vanishes, and the second can be rewritten using the antisymmetry property 1.7, which ultimately leads to

$$[\nabla \cdot \mathbf{F}]_w^C(t, \mathbf{x}) = \int_{\Omega} \mathbf{F}(t, \mathbf{x}') \cdot \nabla w(\mathbf{x} - \mathbf{x}') d\mathbf{x}', \quad (1.11)$$

again with an estimation

$$[\nabla \cdot \mathbf{F}]_w^C(t, \mathbf{x}) = \nabla \cdot \mathbf{F}(t, \mathbf{x}) + \mathcal{O}(h^2), \quad (1.12)$$

valid under circumstances similar to 1.4 - 1.5.

1.2.2 Discrete interpolation

As stated, the core of SPH lies in the particle-based description of a continuum. The term "particles" is used in the following sense: assume that the continuum is a system consisting of N_p (possibly macroscopic) bodies liable to a geometrical description using three generalized coordinates. We call the bodies particles, and we always suppose the coordinates coincide with the coordinates describing the center of inertia of a particle. Moreover, we also neglect any rotational motion of the particles. For a particle a , we denote by \mathbf{x}_a its (generalized) position, \mathbf{u}_a its velocity vector. The density ρ_a , volume V_a and mass m_a of a particle a are linked by the well-known equation⁵

$$\rho_a = \frac{m_a}{V_a} \quad (1.13)$$

The main idea behind the discrete interpolation of physical quantities is to approximate integration by summation. Given an arbitrary field (scalar, vector) $\Phi(t, \mathbf{x})$, we define its discrete interpolation through continuous interpolation as defined in Section 1.2.1.

$$\begin{aligned} [\Phi(t, \mathbf{x})]_w^C &= \int_{\Omega} \Phi(t, \mathbf{x}') w(\mathbf{x} - \mathbf{x}') d\mathbf{x}' \approx \sum_{\mathbf{x}_b} \Phi(t, \mathbf{x}_b) w(\mathbf{x} - \mathbf{x}_b) V_b \\ &:= [\Phi(t, \mathbf{x})]_w^D, \end{aligned} \quad (1.14)$$

where the summation is over all material points (e.g. particles) \mathbf{x}_b . If the interpolation kernel $w(\mathbf{x})$ has a compact support, the sum is reduced only to particles in a certain region. In a less formal but more straightforward way, we have made the following "substitutions":

⁵Here we implicitly work in the Lagrange frame, see 1.4.1. In later sections, we also define density in the Euler frame.

$$\mathbf{x}' \xrightarrow{[\cdot]^D} \mathbf{x}_b \quad (1.15)$$

$$\int_{\Omega} d\mathbf{x}' \xrightarrow{[\cdot]^D} \sum_{\mathbf{x}_b} V_b \quad (1.16)$$

Discrete interpolation of differential operators

Using the definition of discrete interpolation 1.14, the differential operators take the form

$$[\nabla \Phi(t, \mathbf{x})]_w^D = \sum_{\mathbf{x}_b} \Phi(t, \mathbf{x}_b) \nabla w(\mathbf{x} - \mathbf{x}_b) V_b \quad (1.17)$$

$$[\nabla \cdot \mathbf{F}(t, \mathbf{x})]_w^D = \sum_{\mathbf{x}_b} \mathbf{F}(t, \mathbf{x}_b) \cdot \nabla w(\mathbf{x} - \mathbf{x}_b) V_b \quad (1.18)$$

It is natural to define the discrete interpolation error in the following way:

$$E_d[\Phi(t, \mathbf{x})] := \sum_{\mathbf{x}_b} \Phi(t, \mathbf{x}_b) V_b - \int_{\Omega} \Phi(t, \mathbf{x}') d\mathbf{x}' \quad (1.19)$$

As with every approximation technique, finding estimates for $E_d[\cdot]$ is essential. This task is much more complicated than estimating the errors made with the continuous interpolation 1.3 due to the explicit dependence on the position of the particles. Some analysis can be made supposing that the particles occupy, e.g. a regular Cartesian grid, or, by contrast, are distributed randomly. In the case of a Cartesian grid, using the Fourier transform, it can be shown Violeau [2012] that $E_d[\cdot] = \mathcal{O}(h^2)$. In the case of a random distribution of particles, Monte Carlo methods are used and a result $E_d[\cdot] = \mathcal{O}(N_p^{-1/2})$ can be obtained, where N_p stands for the number of particles occupying the region Ω of a continuum Vaughan et al. [2007]. Unfortunately, the typical setting for SPH shows a more disordered configuration than that of a Cartesian grid, but less than that is sufficient for using Monte Carlo methods. Thus, the estimation of discrete interpolation error remains an open question Violeau [2012]. For completeness, we recall that the total error of the interpolation consists of the errors of continuous interpolation 1.3 and discrete interpolation 1.19

In order to obtain the discrete version of the fluid equations, we are interested only in the points \mathbf{x} that coincide with the material points $\mathbf{x}_a = \mathbf{e}_{a,k} x_a^k$. That is, the discrete interpolation of an arbitrary scalar field $\Phi(t, \mathbf{x})$ and an arbitrary vector field $\mathbf{F}(t, \mathbf{x})$ taken at points $\mathbf{x} = \mathbf{x}_a$ can be written, using the standard notation $\Phi_b := \Phi(t, \mathbf{x}_b)$, $r_{ab} := \|\mathbf{x}_{ab}\| := \|\mathbf{x}_a - \mathbf{x}_b\|$, as ⁶

$$[\Phi(t, \mathbf{x}_a)]_w^D = \sum_b \Phi_b w(r_{ab}) V_b \quad (1.20)$$

$$[\mathbf{F}(t, \mathbf{x}_a)]_w^D = \sum_b \mathbf{F}_b w(r_{ab}) V_b, \quad (1.21)$$

where by summing over “b” we mean summing over all material points \mathbf{x}_b . Rewriting equations 1.17 for $\mathbf{x} = \mathbf{x}_a$ while using $\nabla_a = \mathbf{e}_k \frac{\partial}{\partial x_a^k}$ gives

⁶We do not write the time dependence for the sake of simplicity of notation

$$[\nabla\Phi(t, \mathbf{x}_a)]_w^D = \sum_b \Phi_b \nabla_a w(r_{ab}) V_b \quad (1.22)$$

$$[\nabla \cdot \mathbf{F}(t, \mathbf{x}_a)]_w^D = \sum_b \mathbf{F}_b \cdot \nabla_a w(r_{ab}) V_b, \quad (1.23)$$

It is common to rewrite the terms with the nabla operator using the following identity and the notation $\mathbf{e}_{ab} := \frac{1}{r_{ab}} \mathbf{x}_{ab}$, $w(r_{ab}) := w_{ab}$

$$\nabla_a w(r_{ab}) = \mathbf{e}_k \frac{\partial w(r_{ab})}{\partial x_a^k} = -\mathbf{e}_k \frac{\partial w(r_{ab})}{\partial x_b^k} = -\nabla_b w(r_{ab}) = w'(r_{ab}) \mathbf{e}_{ab} = w'_{ab} \mathbf{e}_{ab}, \quad (1.24)$$

which follows from the antisymmetry property of the kernel 1.7 and the chain rule for differentiation. In conclusion, we have arrived at the following results (recall $\Phi(t, \mathbf{r}_a) = \Phi_a$)

$$\Phi_a \approx \sum_b \Phi_b w_{ab} V_b := J(\Phi_a) \quad (1.25)$$

$$\mathbf{F}_a \approx \sum_b \mathbf{F}_b w_{ab} V_b := \mathbf{J}(\mathbf{F}_a) \quad (1.26)$$

$$\nabla\Phi_a \approx \sum_b \Phi_b w'_{ab} \mathbf{e}_{ab} V_b := \mathbf{G}(\Phi_a) \quad (1.27)$$

$$\nabla \cdot \mathbf{F}_a \approx \sum_b \mathbf{F}_b \cdot w'_{ab} \mathbf{e}_{ab} V_b := D(\Phi_a), \quad (1.28)$$

which yields $\forall a$, i.e. for all material points \mathbf{x}_a . From the construction it follows that the operators J, \mathbf{J} approximate the (scalar and tensor) identity operators and \mathbf{G}, D approximate the gradient and divergence operators. In the SPH literature, it is common to adopt a more "lightweight" notation, which, on the other hand, obscures the meaning of the terms Violeau [2012]. It is common to write

$$J_a(\Phi_b) := \sum_b \Phi_b w_{ab} V_b \quad (1.29)$$

$$\mathbf{J}_a(\mathbf{F}_b) := \sum_b \mathbf{F}_b w_{ab} V_b \quad (1.30)$$

$$\mathbf{G}_a(\Phi_b) := \sum_b \Phi_b w'_{ab} \mathbf{e}_{ab} V_b \quad (1.31)$$

$$D_a(\Phi_b) := \sum_b \mathbf{F}_b \cdot w'_{ab} \mathbf{e}_{ab} V_b, \quad (1.32)$$

in the sense that $J_a(\Phi_b) = [\Phi(t, \mathbf{x}_a)]_w^D$, meaning $J_a(\Phi_b)$ is the value of the interpolated field at the material point \mathbf{x}_a etc.

It might seem that we are ready to deploy this formalism to the fundamental equations, which is unfortunately not true. Notice that generally

$$J_a(1) \neq 0 \quad (1.33)$$

$$\mathbf{J}_a(\mathbb{I}) \neq 0 \quad (1.34)$$

$$\mathbf{G}_a(1) \neq 0 \quad (1.35)$$

$$D_a(\mathbb{I}) \neq 0, \quad (1.36)$$

and also for any constant fields. This problem has various solutions, such as the renormalization process explained in Violeau [2012]. However, that approach is rather tedious, and thus we present a different approach, introduced by Monaghan in Monaghan [2005]. Calculus yields the following identities

$$\nabla\Phi = \frac{1}{\rho^k}\nabla(\rho^k\Phi) - \frac{\Phi}{\rho^k}\nabla(\rho^k) \quad (1.37)$$

$$\nabla\cdot\mathbf{F} = \frac{1}{\rho^k}\nabla\cdot(\rho^k\mathbf{F}) - \frac{\mathbf{F}}{\rho^k}\cdot\nabla(\rho^k), \quad (1.38)$$

which we interpolate using the operators \mathbf{G}_a, D_a to obtain

$$(\nabla\Phi)_a \approx \frac{1}{\rho_a^k}\mathbf{G}_a(\rho^k\Phi)_b - \frac{\Phi_a}{\rho_a^k}\mathbf{G}_a(\rho^k)_b \quad (1.39)$$

$$(\nabla\cdot\mathbf{F})_a \approx \frac{1}{\rho_a^k}D_a(\rho^k\mathbf{F})_b - \frac{\mathbf{F}_a}{\rho_a^k}\cdot\mathbf{G}_a(\rho^k)_b \quad (1.40)$$

From the definition of the operators (1.29), it follows

$$\begin{aligned} (\nabla\Phi)_a^k &\approx \frac{1}{\rho_a^k}\sum_b \rho_a^k\Phi_b w'_{ab}\mathbf{e}_{ab}V_b - \frac{\Phi_a}{\rho_a^k}\sum_b \rho_b^k w'_{ab}\mathbf{e}_{ab}V_b \\ &= \frac{1}{\rho_a^{2k}}\sum_b (\rho_b\rho_a)^k\Phi_b w'_{ab}\mathbf{e}_{ab} - \frac{1}{\rho_a^{2k}}\sum_b (\rho_b\rho_a)^k\Phi_a w'_{ab}\mathbf{e}_{ab}V_b = -\frac{1}{\rho_a^{2k}}\sum_b (\rho_b\rho_a)^k\Phi_{ab} w'_{ab}\mathbf{e}_{ab}V_b := \mathbf{G}_a^k, \end{aligned}$$

while introducing the notation $\Phi_{ab} := \Phi_a - \Phi_b$. Using the same procedure, the formula for divergence becomes

$$(\nabla\cdot\mathbf{F})_a^k \approx -\frac{1}{\rho_a^{2k}}\sum_b (\rho_a\rho_b)^k\mathbf{F}_{ab} w'_{ab}\mathbf{e}_{ab}V_b := D_a^k,$$

where again $\mathbf{F}_{ab} := \mathbf{F}_a - \mathbf{F}_b$. The relations above define two sets of discretized gradient and divergence operators \mathbf{G}_a^k, D_a^k . Later, we will make use of the operators for $k = 1$, i.e.

$$\mathbf{G}_a^1(\Phi_b) = -\frac{1}{\rho_a}\sum_b m_b\Phi_{ab} w'_{ab}\mathbf{e}_{ab} \quad (1.41)$$

$$D_a^1(\mathbf{F}_b) = -\frac{1}{\rho_a}\sum_b m_b\mathbf{F}_{ab}\cdot w'_{ab}\mathbf{e}_{ab}, \quad (1.42)$$

where we substituted the volume for mass using (1.13). Due to the differences in the above equations (i.e. $\Phi_{ab}, \mathbf{F}_{ab}$) we have

$$\mathbf{G}_a^k(1) = 0$$

$$D_a^k(\mathbb{I}) = 0$$

1.3 Discrete version of fluid equations

The formalism adopted in the previous sections allows us to derive discretized versions of fluid equations. As they are fundamental and the goal of this work lies elsewhere, we do not provide a derivation of them. If interested, see any book on continuum mechanics, e.g. Gurtin and Drugan [1984].

1.3.1 Discrete continuity equation

We begin with the continuity equation (conservation of mass) in differential form:

$$\frac{D\rho}{Dt} + \rho \nabla \cdot \mathbf{u} = 0, \quad (1.43)$$

the material derivative operator being

$$\frac{Dt}{Dt} = \begin{cases} \frac{\partial}{\partial t} + \nabla \cdot \mathbf{u}, & \text{in the Euler picture} \\ \frac{\partial}{\partial t}, & \text{in the Lagrange picture} \end{cases} \quad (1.44)$$

Clearly, SPH is an Lagrangian method, that is, the particles represent material points in a co-moving reference frame. For more discussion on the differences between the Euler and the Lagrange frame, see 1.4.1. Discretising the divergence operator using the operator D_a^1 defined in eq. (1.41) gives⁷

$$\frac{d}{dt}\rho_a = \sum_b m_b \mathbf{u}_{ab} \cdot w'_{ab} \mathbf{e}_{ab}, \forall a \quad (1.45)$$

The equation above is not the only possible way to discretise the continuity equation. For instance, we could have used the D_a^k as defined in eq (1.39) for any other k . Nevertheless, the form of the equation (1.45) is the commonly used form Monaghan [2005] and also is the version which we will come across once again in the section 1.4.5.

1.3.2 Discrete Euler equations

Recall the Navier-Stokes equations for viscous incompressible Newtonian fluids in a homogeneous gravitational field Gurtin and Drugan [1984]

$$\rho \frac{D\mathbf{u}}{Dt} = -\nabla p + \mu \nabla \cdot \nabla \mathbf{u} + \rho \mathbf{g}, \quad (1.46)$$

where p denotes the pressure, μ is the (dynamic) viscosity and \mathbf{g} is the gravitational acceleration. When the viscous forces may be neglected, N-S equations take the form

$$\frac{D\mathbf{u}}{Dt} = -\frac{1}{\rho} \nabla p + \mathbf{g} \quad (1.47)$$

⁷Note that we write $\frac{d}{dt}$ instead of $\frac{\partial}{\partial t}$. While it is true that in the Lagrangian frame the material derivative equals the standard partial derivative, in the ‘‘particle notation’’ of SPH we specify by using the lower index a a particular particle, so technically the function ρ_a is only a function of time.

Equations (1.47) are called Euler equations and are traditionally used in meteorology. Using the \mathbf{G}_a^1 operator (1.41) to discretize the grad operator in the Euler equations reads as

$$\frac{d}{dt}\mathbf{u}_a = -\sum_b m_b \left(\frac{p_a}{\rho_a^2} + \frac{p_b}{\rho_b^2} \right) w'_{ab} \mathbf{e}_{ab} + \mathbf{g}_a, \forall a \quad (1.48)$$

1.3.3 The complete WCSPH scheme

Barotropic equation of state for the pressure

To close the equations presented in the previous sections, an equation of state must be specified. Since the only intensive thermodynamic quantity presented so far is the pressure, a state equation for pressure (the thermal state equation) is sought. The standard choice of the thermal state equation in modeling weakly compressible flows (see, e.g., Violeau [2012]) was derived by Murnaghan in 1944 in Murnaghan [1944]. For the sake of completeness, we cover the derivation also here, but in later sections, we will predominantly use a different thermal state equation (of an ideal gas).

Define the fluid incompressibility modulus

$$K := -\rho \frac{\partial p}{\partial \rho},$$

which is a response coefficient that measures the effect of density on pressure. For fluids with relatively small density variations ⁸ the previous term can be expanded via its Taylor series

$$\begin{aligned} K &= -K_0 - \gamma p + \mathcal{O}(p^2), \\ K_0 &:= \left(\rho \frac{\partial p}{\partial \rho} \right) \Big|_{p=0} \\ \gamma &:= \frac{\partial K}{\partial p} \Big|_{p=0} \end{aligned}$$

Neglecting all the nonlinear terms in p leads to a differential equation for $p = p(\rho)$

$$\rho \frac{dp}{d\rho} - \gamma p - K_0 = 0,$$

with a solution

$$p(\rho) = C \rho^\gamma - \frac{K_0}{C\gamma},$$

where C is an integration constant. Solving for the root of the previous function gives

$$\rho_0 := \left(\frac{K_0}{\gamma} \right)^{\frac{1}{\gamma}} \quad (1.49)$$

⁸The formula holds well for the relative volume variations lesser than $\approx 10\%$ Violeau [2012]

which we define as a reference density ρ_0 . Introducing $c := \sqrt{K_0/\rho_0}$ as the speed of sound in the fluid leads to the following equation of state

$$p(\rho) = \frac{\rho_0 c^2}{\gamma} \left[\left(\frac{\rho}{\rho_0} \right)^\gamma - 1 \right], \quad (1.50)$$

as derived in Murnaghan [1944].

Complete equations

Finally, combining equations (1.45), (1.48), (1.50) gives the equations for modelling weakly compressible flows using the SPH method as follows

$$\frac{d}{dt} \rho_a = \sum_b m_b \mathbf{u}_{ab} \cdot w'_{ab} \mathbf{e}_{ab}, \quad (1.51a)$$

$$\frac{d}{dt} \mathbf{u}_a = - \sum_b m_b \left(\frac{p_a}{\rho_a^2} + \frac{p_b}{\rho_b^2} \right) w'_{ab} \mathbf{e}_{ab} + \mathbf{g}_a, \forall a \quad (1.51b)$$

$$p(\rho) = \frac{\rho_0 c^2}{\gamma} \left[\left(\frac{\rho}{\rho_0} \right)^\gamma - 1 \right], \quad (1.51c)$$

1.4 SPH equations as a Hamiltonian system

To conclude this chapter, we present a different approach to deriving the SPH equations (1.51a) using the elegant framework of Hamiltonian systems. The main reason for this approach is to discover the Hamiltonianity of the previously derived system of equations. It will also be shown that a slightly different system of equations is even symplectic; we are interested in such systems as they possess advantageous numerical properties.

Another reason to exploit Hamiltonian mechanics roots in thermodynamics (remember how the fundamental equations in statistical physics are obtained using Hamiltonian mechanics). Within this framework, including quantities such as entropy and dissipation in the SPH equations is not difficult. Those thermodynamical considerations are indispensable when dealing with dissipative systems (e.g. viscous flows). Even though we aim to use the standard Euler equations, we will later on face a need for a more thermodynamically-sophisticated formalism. Notice how for example we have not included temperature in our considerations; this will prove insufficient when dealing with atmospheric systems.

Unfortunately, precise formulation of such a theory requires deeper knowledge of continuum and non-equilibrium thermodynamics; the topic of this text lies elsewhere. Thus, when the need arises, we kindly draw from the work done in Kincl et al. [2023a]. We stress that the goal of this section is not to provide a comprehensive analysis of the topic. Only facts important to our research goal are presented here.

1.4.1 Lagrange and Euler picture

Continuum mechanics, a vast field of classical physics, can be described from different frames of reference. In all physics, inertial frames possess a significant role. In continuum mechanics, an inertial frame is called the Euler frame (also called the Euler picture, the spatial frame). It is common to use the Euler picture especially in fluid mechanics: imagine a flow of fluid described by a velocity field $\mathbf{u}(t, \mathbf{x})$, that is, a function that assigns the vector $\mathbf{u}(t, \mathbf{x})$ to time t and the *Eulerian coordinates* \mathbf{x} . The Eulerian coordinates \mathbf{x} represent a fixed point in space, through which, for example, the fluid might flow.

Another means of description are possible. Suppose that we fix the origin of the frame of reference so that it coincides with some material point \mathbf{X} of the continuum at some reference time. Then, throughout time evolution (deformation, etc.), the point \mathbf{X} does not change with respect to this special (non-inertial) frame. This frame is called the Lagrangian frame (also the Lagrangian picture, material frame, and reference frame), and the coordinate \mathbf{X} is the *Lagrangian coordinate*. The Lagrange picture is often used in solid mechanics: imagine a deformation of a body. The Lagrangian coordinates \mathbf{X} represent a material point (i.e., a part of the body) that, for example, undergoes deformation.

It is good practice to denote all Lagrangian variables (defined in the Lagrangian frame) with uppercase letters and to denote all Eulerian variables (defined in the Euler frame) with lowercase letters; we will stick to this convention in what follows. The fundamental question arises: How do we describe the relationship of both pictures? We imagine that a material point in the current configuration at a particular time t , as described by the Eulerian variables \mathbf{x} , is some material point \mathbf{X} from the reference configuration. Thus, there must exist a mapping $\mathbf{x}(t, \mathbf{X})$ from the Lagrange frame to the Euler frame.

1.4.2 Choice of the manifold

As in classical theoretical mechanics, the mechanical state of a material point \mathbf{X} at a time t can be described by its position $\mathbf{x}(t, \mathbf{X})$ and velocity $\dot{\mathbf{x}}(t, \mathbf{X})$ (Lagrangian mechanics) or by its position $\mathbf{x}(t, \mathbf{X})$ and its momentum density $\mathbf{M}(t, \mathbf{X})$ (i.e., the momentum of the material point per volume (Lagrangian) $d\mathbf{X}$). Pavelka et al. [2020]. We are looking for a Hamiltonian description and thus choose the position $\mathbf{x}(t, \mathbf{X})$ and the momentum density $\mathbf{M}(t, \mathbf{X})$ to be the state variables.

The Eulerian positions form the configuration manifold, whereas the momentum densities form a cotangent bundle (dual space to the tangent bundle) of that manifold Pavelka et al. [2020]. Such a structure naturally provides a Poisson bracket.

1.4.3 Canonical Poisson bracket in the Lagrangian frame

Seeking time evolution, we are interested in finding a Poisson bracket and an energy functional. Given two arbitrary functionals $F(\mathbf{x}(t, \mathbf{X}), \mathbf{M}(t, \mathbf{X}))$ of the Lagrangian variables, we define its Poisson bracket (see Pavelka et al. [2020])

$$\{F, G\}^{(L)} := \int \left(\frac{\delta F}{\delta x^i(\mathbf{X})} \frac{\delta G}{\delta M_i(\mathbf{X})} - \frac{\delta F}{\delta M_i(\mathbf{X})} \frac{\delta G}{\delta x^i(\mathbf{X})} \right) d\mathbf{X}, \quad (1.52)$$

where the superscript stands for Lagrangian frame and for brevity, we have also omitted the explicit time dependency for the rest of this section. The derivatives under the integral sign are functional derivatives. Since the aim of the thesis does not lie in this topic, we kindly advise the reader to see the appendix Pavelka et al. [2018]; for our use, it suffices that the functional derivative yields

$$\left\langle \frac{\delta F}{\delta f}, \phi \right\rangle = dF(f, \phi), \forall \phi \in \mathcal{D}, \text{ i.e.} \quad (1.53a)$$

$$\left. \frac{d}{ds} \right|_{s=0} F(f + sh) = \left\langle \frac{\delta F}{\delta f}, h \right\rangle, \forall h \in \mathcal{D}, \quad (1.53b)$$

where $\langle \cdot, \cdot \rangle$ is the duality in the sense of distributions, $dF(f, \phi)$ represents the Frechet differential of the functional F with respect to the function f at the point ϕ , \mathcal{D} is the space of infinitely smooth functions with a compact support (in some region based on context). The first line can be interpreted as that the functional derivative is a distribution corresponding to the Frechet differential.

It should be checked that the relation (1.52) indeed defines a Poisson bracket, an antilinear bivector satisfying the Jacobi identity and the Leibniz rule. However, since these proofs require a more profound knowledge of the functional derivatives, we refer again to Pavelka et al. [2020]. As in classical mechanics, the Hamiltonian evolution of an arbitrary functional of the Lagrangian variables can then be expressed as follows.

$$\frac{d}{dt} F = \{F, E\}^{(L)}, \quad (1.54)$$

where E is the functional of total energy. For example, we can examine the evolution of the Lagrangian state variables.

Hamiltonian equations for Lagrangian state variables

Let $F(\mathbf{x}(\mathbf{X}), \mathbf{M}(\mathbf{X}))$ be any functional of the state variables and use the relation above

$$\frac{d}{dt} F(\mathbf{x}(\mathbf{X}), \mathbf{M}(\mathbf{X})) = \{F, E\}^{(L)} = \int \left(\frac{\delta F}{\delta x^i(\mathbf{X})} \frac{\delta E}{\delta M_i(\mathbf{X})} - \frac{\delta F}{\delta M_i(\mathbf{X})} \frac{\delta E}{\delta x^i(\mathbf{X})} \right) d\mathbf{X},$$

by using the chain differentiation rule for function(al) derivatives Pavelka et al. [2020], we on the other hand obtain

$$\frac{d}{dt} F(\mathbf{x}(\mathbf{X}), \mathbf{M}(\mathbf{X})) = \int \left(\frac{\delta F}{\delta x^i(\mathbf{X})} \frac{\partial x^i}{\partial t} + \frac{\delta F}{\delta M_i(\mathbf{X})} \frac{\partial M_i}{\partial t} \right) d\mathbf{X}$$

The equations above must be equal for an arbitrary functional F so we can conclude

$$\frac{\partial}{\partial t} x^i(\mathbf{X}) = \frac{\delta E}{\delta M_i(\mathbf{X})}, \quad (1.55)$$

$$\frac{\partial}{\partial t} M_i(\mathbf{X}) = -\frac{\delta E}{\delta x_i(\mathbf{X})} \quad (1.56)$$

The equations (1.55) represent the Hamilton equations of continuum mechanics. However, we still need to prescribe the energy functional.

Assume that the total energy consists of kinetic energy and internal energy. It is most convenient to obtain the density of the internal energy in the Eulerian variables, that is, $\epsilon = \epsilon(\rho(\mathbf{x}))$, where ϵ is the internal energy density in the Euler frame and ρ is the mass density, also in the Euler frame. We seek the evolution of Lagrangian variables, so we have to transform the Eulerian variables using the Jacobian

$$d\mathbf{x} = \det \frac{\partial \mathbf{x}}{\partial \mathbf{X}} d\mathbf{X}$$

and so

$$E^{(L)} = \int \left(\frac{\mathbf{M}^2}{2\rho^{(L)}} + \det \frac{\partial \mathbf{x}}{\partial \mathbf{X}} \epsilon(\rho(\mathbf{x}(\mathbf{X}))) \right) d\mathbf{X}, \quad (1.57)$$

where $\rho^{(L)}$ is the Lagrangian mass density. We still need to transform the Eulerian mass density ρ to the Lagrangian frame, but we will not make the transformation now for simplicity.

1.4.4 The SPH Poisson bracket

Let Ω be a region of the continuum (for example, a body). Define $\{\Omega_a\}$ to be a partition of Ω such that $\Omega = \cup_a \Omega_a$, $\Omega_a \cap \Omega_b = \emptyset$ if $a \neq b$ and $V_a = \int_{\Omega_a} d\mathbf{X}$ to be the volume of each Ω_a . Later, we will call Ω_a a (SPH) particle. Next, define the normalized characteristic function of Ω_a , that is, $\chi_a(\mathbf{X}) = 1/V_a$, if $\mathbf{X} \in \Omega_a$, and $\chi_a(\mathbf{X}) = 0$ if $\mathbf{X} \notin \Omega_a$. Finally, define the position and momentum of the particle using the relations⁹

$$\mathbf{x}_a = \int \mathbf{x}(\mathbf{X}) \chi_a(\mathbf{X}) d\mathbf{X} \quad (1.58a)$$

$$\mathbf{M}_a = \int \mathbf{M}(\mathbf{X}) \chi_a(\mathbf{X}) V_a d\mathbf{X}, \quad (1.58b)$$

Aiming to obtain the ‘‘SPH Poisson bracket’’, i.e., a Poisson bracket generating the SPH equations, we define the equations (1.58a) to be the SPH state variables. Now consider two arbitrary functionals of these state variables $F(\mathbf{x}_a, \mathbf{M}_b)$, $G(\mathbf{x}_a, \mathbf{M}_b)$ and insert them into the continuum Poisson bracket (1.52). Once again, deploying the chain rule (for functional derivatives) yields

$$\begin{aligned} \{F, G\}^{(L)} &= \int \left(\frac{\delta F}{\delta x^i(\mathbf{X})} \frac{\delta G}{\delta M_i(\mathbf{X})} - \frac{\delta F}{\delta M_i(\mathbf{X})} \frac{\delta G}{\delta x^i(\mathbf{X})} \right) = \\ &= \sum_a \sum_b \int \left(\left[\frac{\partial F}{\partial x_a^j} \frac{\delta x_a^j}{\delta x^i(\mathbf{X})} + \frac{\partial F}{\partial M_{b,j}} \frac{\delta M_{b,j}}{\delta x^i(\mathbf{X})} \right] \left[\frac{\partial G}{\partial M_{b,j}} \frac{\delta M_{b,j}}{\delta M_i(\mathbf{X})} + \frac{\partial G}{\partial x_a^j} \frac{\delta x_a^j}{\delta M_i(\mathbf{X})} \right] - \right. \\ &\quad \left. \left[\frac{\partial F}{\partial M_{b,j}} \frac{\delta M_{b,j}}{\delta M_i(\mathbf{X})} + \frac{\partial F}{\partial x_a^j} \frac{\delta x_a^j}{\delta M_i(\mathbf{X})} \right] \left[\frac{\partial G}{\partial x_a^j} \frac{\delta x_a^j}{\delta x^i(\mathbf{X})} + \frac{\partial G}{\partial M_{b,j}} \frac{\delta M_{b,j}}{\delta x^i(\mathbf{X})} \right] \right) d\mathbf{X} \quad (1.59) \end{aligned}$$

⁹Notice the multiplication by V_a , since $\mathbf{M}(\mathbf{X})$ is the (Eulerian) momentum density per Lagrangian volume.

Where the summation over a, b means a summation over all particles ¹⁰ To evaluate the functional derivatives, we use (1.53a) in the form

$$\begin{aligned} \left\langle \frac{\delta x_a^j}{\delta x^i(\mathbf{X})}, h \right\rangle &= \int \frac{\delta x_a^j}{\delta x^i(\mathbf{X})} h \, d\mathbf{X} = \left. \frac{d}{ds} \right|_{s=0} x_a^j(x^i + sh) = \\ &= \left. \frac{d}{ds} \right|_{s=0} \int \delta_i^j(x^i(\mathbf{X}) + sh) \chi_a(\mathbf{X}) \, d\mathbf{X} = \int \delta_i^j \chi_a(\mathbf{X}) h \, d\mathbf{X}, \end{aligned}$$

where the δ_i^j appears because of the fact that due to (1.58a) the coordinate x_a^j is only a function of $x^j(\mathbf{X})$ (not other coordinates). Since this equality holds $\forall h \in \mathcal{D}$, we deduce that

$$\frac{\delta x_a^j}{\delta x^i(\mathbf{X})} = \delta_i^j \chi_a(\mathbf{X}),$$

and since x_a^j is by its definition (1.58a) only a function of \mathbf{x} , all the functional derivatives with respect to $M_i(\mathbf{X})$ are identically zero. The same analysis can be performed by changing $x_a^j \leftrightarrow M_{b,j}$ to obtain the following.

$$\frac{\delta M_{b,j}}{\delta M_i(\mathbf{X})} = \delta_i^j \chi_b(\mathbf{X}) V_b$$

Using these facts to simplify the equation (1.59) gives the following result.

$$\begin{aligned} \{F(\mathbf{x}_a, \mathbf{M}_b), G(\mathbf{x}_a, \mathbf{M}_b)\}^{(L)} &= \\ &= \sum_a \sum_b \int \left(\frac{\partial F}{\partial x_a^i} \frac{\partial G}{\partial M_{b,i}} \chi_a(\mathbf{X}) \chi_b(\mathbf{X}) V_b - \frac{\partial F}{\partial M_{b,i}} \frac{\partial G}{\partial x_a^i} \chi_a(\mathbf{X}) \chi_b(\mathbf{X}) V_b \right) d\mathbf{X} = \\ &= \sum_a \sum_b \left(\frac{\partial F}{\partial x_a^i} \frac{\partial G}{\partial M_{b,i}} - \frac{\partial F}{\partial M_{b,i}} \frac{\partial G}{\partial x_a^i} \right) \int \chi_a(\mathbf{X}) \chi_b(\mathbf{X}) V_b \, d\mathbf{X}, \end{aligned}$$

using the definition of a normalised characteristic function and the fact that the partition of Ω is (pairwise) disjoint, one can simplify the integral

$$\int \chi_a(\mathbf{X}) \chi_b(\mathbf{X}) V_b \, d\mathbf{X} = \int \chi_a^2(\mathbf{X}) V_a \, d\mathbf{X} = \int_{\Omega_a} \frac{1}{V_a^2} V_a \, d\mathbf{X} = \frac{1}{V_a} \int_{\Omega_a} d\mathbf{X} = 1,$$

which leads to

$$\sum_a \sum_b \left(\frac{\partial F}{\partial x_a^i} \frac{\partial G}{\partial M_{b,i}} - \frac{\partial F}{\partial M_{b,i}} \frac{\partial G}{\partial x_a^i} \right) \int \chi_a(\mathbf{X}) \chi_b(\mathbf{X}) V_b \, d\mathbf{X} = \sum_a \left(\frac{\partial F}{\partial x_a^i} \frac{\partial G}{\partial M_{a,i}} - \frac{\partial F}{\partial M_{a,i}} \frac{\partial G}{\partial x_a^i} \right) \Big|$$

This is exactly the definition of the SPH Poisson bracket ¹¹; that is, for arbitrary functionals F, G of the SPH state variables, we set

¹⁰If the functionals do not depend on some of the variables, then the partial derivatives are zero, and we have added only zeros to the result

¹¹In the Lagrangian frame

$$\{F, G\}^{(SPH)} := \sum_a \left(\frac{\partial F}{\partial x_a^i} \frac{\partial G}{\partial M_{a,i}} - \frac{\partial F}{\partial M_{a,i}} \frac{\partial G}{\partial x_a^i} \right) \quad (1.60)$$

There are several interesting facts to be aware about the SPH Poisson bracket. Mainly, it is identical to that of classical mechanics (of particles). This agrees well with the “particle interpretation” and checks that the relations truly define a Poisson bracket (antilinear bivector satisfying the Jacobi identity and the Leibniz rule). Also, compare the derivation with the process of interpolation described in section 1.2.

- The functions (state variables) $\mathbf{x}(\mathbf{X})$, $\mathbf{M}(\mathbf{X})$ have been simplified through an integration (1.58a) over a subregion of the continuum. This is similar to the continuous interpolation (1.2).
- Integration over a “continuous” region (i.e., over a continuous variable) in the Poisson bracket (1.52) has been simplified to a summation over the particles (i.e. a “discrete region”) (1.60). Again, compare this to the discrete interpolation (1.14) or (1.15) schematically

1.4.5 Hamilton equations induced by the SPH Poisson bracket

The SPH energy functional

In the previous sections, we have concluded that to write down the evolution equations, we need some state variables, a Poisson bracket, and an energy functional. Only the last ingredient is missing: the energy functional. The relation (1.57) defines the energy of the continuum. Let us try to recreate such a relation using the SPH variables. No difficulty poses the mass of a particle

$$m_a = \int \rho^{(L)}(\mathbf{X}) \chi_a(\mathbf{X}) d\mathbf{X}, \quad (1.61)$$

and using the definition of the particle volume V_a one can also define the SPH density in the *Lagrange frame*

$$\rho_a^{(L)} = \frac{m_a}{V_a} \quad (1.62)$$

However, the relation (1.57) also calls for the density in the *Euler frame* (as well as for the mapping $\mathbf{X} \mapsto \mathbf{x}(t, \mathbf{X})$). In the material configuration, the SPH density is easy to define, as it is the density of the particle with which the frame moves. In the current configuration, the SPH density at a point in space, with respect to the fixed frame, needs to take into account that the particles around are moving. Thus, the density must be determined by the attributes of the particles at a certain neighborhood of that point, ergo, we require the idea of an interpolation kernel. With enough knowledge of the matter, let us immediately define the SPH density in the Euler frame.

$$\rho_a = \sum_b m_b w_{ab} \quad (1.63)$$

This quantity is indeed a mass density, as the dimension of w_{ab} is meter⁻ⁿ, where n is the dimension of the Euclidean space. Using the discrete interpolation scheme (1.15) (we need to sum over the particles) and the rule for volume transformation, that is

$$\rho \, d\mathbf{x} = \rho \det \frac{\partial \mathbf{x}}{\partial \mathbf{X}} \, d\mathbf{X} = \rho^{(L)} \, d\mathbf{X} \Rightarrow \det \frac{\partial \mathbf{x}}{\partial \mathbf{X}} = \frac{\rho^{(L)}}{\rho},$$

the SPH energy becomes

$$E^{(SPH)} = \sum_a \left(\frac{\mathbf{M}_a^2}{2\rho_a^{(L)}} + \frac{\rho_a^{(L)}}{\rho_a} \epsilon(\rho_a) \right) V_a = \sum_a \left(\frac{\mathbf{M}_a^2}{2m_a} + \frac{m_a}{\rho_a} \epsilon(\rho_a) \right) \quad (1.64)$$

Evolution equations

We are ready to construct the SPH version of the Hamilton equations. That is,

$$\frac{d}{dt} x_a^i = \{x_a^i, E^{(SPH)}\}^{(SPH)} = \sum_b \left(\frac{\partial x_a^i}{\partial x_b^j} \frac{\partial E}{\partial M_{b,j}} - \frac{\partial x_a^i}{\partial M_{b,j}} \frac{\partial E}{\partial x_b^j} \right) \quad (1.65a)$$

$$\frac{d}{dt} M_{a,i} = \{M_{a,i}, E^{(SPH)}\}^{(SPH)} = \sum_b \left(\frac{\partial M_{a,i}}{\partial x_b^j} \frac{\partial E}{\partial M_{b,j}} - \frac{\partial M_{a,i}}{\partial M_{b,j}} \frac{\partial E}{\partial x_b^j} \right), \quad (1.65b)$$

$$(1.65c)$$

where we write $E \equiv E^{(SPH)}$ for brevity. Partial derivatives of the state variables with respect to one another are

$$\frac{\partial x_a^i}{\partial x_b^j} = \frac{\partial M_{a,i}}{\partial M_{b,j}} = \delta_j^i \delta_b^a,$$

whereas the mixed derivatives of the state variables are identically zero. For the derivatives of the energy, we write

$$\begin{aligned} \frac{\partial}{\partial x_b^j} E &= \frac{\partial}{\partial x_b^j} \sum_c \left(\frac{\mathbf{M}_c^2}{2m_c} + \frac{m_c}{\rho_c} \epsilon(\rho_c) \right) = \sum_c m_c \epsilon(\rho_c) \frac{\partial}{\partial x_b^j} \left(\frac{1}{\rho_c} \right) + \sum_c \frac{m_c}{\rho_c} \frac{\partial}{\partial x_b^j} \epsilon(\rho_c) = \\ &= \sum_c m_c \epsilon(\rho_c) \frac{\partial}{\partial x_b^j} \left(\frac{1}{\sum_d m_d w(\|\mathbf{x}_c - \mathbf{x}_d\|)} \right) + \sum_c \frac{m_c}{\rho_c} \epsilon'(\rho_c) \frac{\partial}{\partial x_b^j} \sum_d m_d w(\|\mathbf{x}_c - \mathbf{x}_d\|) = \\ &= \sum_c m_c \epsilon(\rho_c) \frac{-1}{\left(\sum_d m_d w(\|\mathbf{x}_c - \mathbf{x}_d\|) \right)^2} \sum_d m_d w'(\|\mathbf{x}_c - \mathbf{x}_d\|) \frac{\partial}{\partial x_b^j} \sqrt{\sum_k (x_c^k - x_d^k)^2} + \\ &\quad + \sum_c \frac{m_c}{\rho_c} \epsilon'(\rho_c) \sum_d m_d w'(\|\mathbf{x}_c - \mathbf{x}_d\|) \frac{\partial}{\partial x_b^j} \sqrt{\sum_k (x_c^k - x_d^k)^2} = \\ &= - \sum_c m_c \epsilon(\rho_c) \frac{1}{\rho_c^2} \sum_d m_d w'(\|\mathbf{x}_c - \mathbf{x}_d\|) \sum_k \frac{x_c^k - x_d^k}{\|\mathbf{x}_c - \mathbf{x}_d\|} \delta^{jk} (\delta_{bc} - \delta_{bd}) + \\ &\quad + \sum_c \frac{m_c}{\rho_c} \epsilon'(\rho_c) \sum_d m_d w'(\|\mathbf{x}_c - \mathbf{x}_d\|) \sum_k \frac{x_c^k - x_d^k}{\|\mathbf{x}_c - \mathbf{x}_d\|} \delta^{jk} (\delta_{bc} - \delta_{bd}) \\ &= \left[\sum_c \left(\frac{m_c}{\rho_c} \epsilon'(\rho_c) - m_c \epsilon(\rho_c) \frac{1}{\rho_c^2} \right) \right] \left[\sum_d m_d w'(\|\mathbf{x}_c - \mathbf{x}_d\|) \frac{x_c^j - x_d^j}{\|\mathbf{x}_c - \mathbf{x}_d\|} (\delta_{bc} - \delta_{bd}) \right], \end{aligned}$$

using the notation from section 1.2.2 and splitting the sum in two parts corresponding to $b=c$ and $b=d$ respectively reads as

$$\begin{aligned}
&= \left[\sum_c \left(\frac{m_c}{\rho_c} \epsilon'(\rho_c) - m_c \epsilon(\rho_c) \frac{1}{\rho_c^2} \right) \right] \left[\sum_d m_d w'_{cd} e_{cd}^j (\delta_{bc} - \delta_{bd}) \right] = \\
&= \left(\frac{m_b}{\rho_b} \epsilon'(\rho_b) - \frac{m_b}{\rho_b^2} \epsilon(\rho_b) \right) \sum_d m_d w'_{bd} e_{bd}^j - \sum_c \left(\frac{m_c}{\rho_c} \epsilon'(\rho_c) - \frac{m_c}{\rho_c^2} \epsilon(\rho_c) \right) m_b w'_{cb} e_{cb}^j = \\
&= \sum_d \left(\frac{m_b}{\rho_b} \epsilon'(\rho_b) - \frac{m_b}{\rho_b^2} \epsilon(\rho_b) \right) m_d w'_{bd} e_{bd}^j + \sum_c \left(\frac{m_c}{\rho_c} \epsilon'(\rho_c) - \frac{m_c}{\rho_c^2} \epsilon(\rho_c) \right) m_b w'_{bc} e_{bc}^j = \\
&= \sum_c \left(\frac{m_b}{\rho_b} \epsilon'(\rho_b) - \frac{m_b}{\rho_b^2} \epsilon(\rho_b) \right) m_c w'_{bc} e_{bc}^j + \sum_c \left(\frac{m_c}{\rho_c} \epsilon'(\rho_c) - \frac{m_c}{\rho_c^2} \epsilon(\rho_c) \right) m_b w'_{bc} e_{bc}^j = \\
&= \sum_c \left[m_c \frac{m_b}{\rho_b^2} \left(-\epsilon(\rho_b) + \rho_b \epsilon'(\rho_b) \right) + m_b \frac{m_c}{\rho_c^2} \left(-\epsilon(\rho_c) + \rho_c \epsilon'(\rho_c) \right) \right] w'_{bc} e_{bc}^j
\end{aligned}$$

where we exploited $e_{cb}^j = -e_{bc}^j$, $w'_{ab} = w'_{ba}$. Defining the pressure of a particle d by the relation Kincl et al. [2023a]

$$p_d = -\epsilon(\rho_d) + \rho_d \epsilon'(\rho_d) = -\epsilon(\rho_d) + \rho_d \frac{\partial \epsilon}{\partial \rho_d}, \quad (1.66)$$

further simplifies the equalities above to obtain finally

$$\frac{\partial E}{\partial x_b^j} = \sum_c \left(\frac{m_c m_b}{\rho_b^2} p_b + \frac{m_c m_b}{\rho_c^2} p_c \right) w'_{bc} e_{bc}^j$$

For the derivatives with respect to momentum, we write

$$\frac{\partial}{\partial M_{b,j}} E = \frac{\partial}{\partial M_{b,j}} \sum_c \left(\frac{\mathbf{M}_c^2}{2m_c} + \frac{m_c}{\rho_c} \epsilon(\rho_c) \right) = \sum_c \frac{1}{2m_c} \frac{\partial}{\partial M_{b,j}} 2M_{c,k} \delta_{jk} \delta_{bc} = \frac{M_{b,j}}{m_b}$$

Combining all the above relations yields

$$\frac{d}{dt} x_a^i = \sum_b \left(\delta_j^i \delta_b^a \frac{M_{b,j}}{m_b} - 0 \right) = \frac{M_{a,i}}{m_a},$$

$$\frac{d}{dt} M_a^i = \sum_b \left(0 - \delta_j^i \delta_b^a \sum_c \left[\frac{m_c m_b}{\rho_b^2} p_b + \frac{m_c m_b}{\rho_c^2} p_c \right] w'_{bc} e_{bc}^j \right) = - \sum_c \left(\frac{m_c m_a}{\rho_a^2} p_a + \frac{m_c m_a}{\rho_c^2} p_c \right) w'_{ac} e_{ac}^i$$

These evolution equations represent the Hamilton canonical equations of the SPH state variables, together with the density relation (1.63) they define a system of ordinary differential equations analogous to the WCSPH scheme (1.51a).

$$\frac{d}{dt} \mathbf{x}_a = \frac{\mathbf{M}_a}{m_a}, \quad (1.67a)$$

$$\frac{d}{dt} \mathbf{M}_a = - \sum_b \left(\frac{m_a m_b}{\rho_a^2} p_a + \frac{m_a m_b}{\rho_b^2} p_b \right) w'_{ab} \mathbf{e}_{ab}, \quad (1.67b)$$

$$\rho_a = \sum_b m_b w_{ab} \quad (1.67c)$$

This system is Hamiltonian, as it is generated by a Poisson bracket (1.60). It must be noted that this is not a unique way to express the SPH equations as a Hamiltonian system. In the section 1.2.2, we have seen numerous ways to discretize the operators, thus leading to multiple formulations of the system. Such an ambiguity remains even when opting for this alternative derivation.

Mainly, the above set of equations is not the same as (1.51a). The real difference lies in the treatment of density: whereas the “classical” SPH prescribes an evolution equation for density, the Hamilton canonical equations above only evolve positions and momenta and set the density as a function of these state variables¹². Inspired by the classical SPH, let us find an evolution equation for the density, using a generic Hamiltonian evolution (1.54)

$$\begin{aligned} \frac{d}{dt}\rho_a &= \{\rho_a, E\}^{(SPH)} = \sum_b \left(\frac{\partial \rho_a}{\partial x_b^j} \frac{\partial E}{\partial M_{b,j}} - \frac{\partial \rho_a}{\partial M_{b,j}} \frac{\partial E}{\partial x_b^j} \right) = \sum_b \left(\frac{M_{b,j}}{m_b} \frac{\partial}{\partial x_b^j} \sum_c m_c w_{ac} - 0 \right) \\ &= \sum_b \left(\frac{M_{b,j}}{m_b} \sum_c m_c w'_{ac} e_{ac}^k \delta_j^k (\delta_{ba} - \delta_{bc}) \right) = \sum_b \sum_c \left(\frac{M_{b,j}}{m_b} m_c w'_{ac} e_{ac}^j (\delta_{ba} - \delta_{bc}) \right) \\ &= \sum_c \left(\frac{M_{a,j}}{m_a} m_c w'_{ac} e_{ac}^j \right) - \sum_c \left(\frac{M_{c,j}}{m_c} m_c w'_{ac} e_{ac}^j \right) = \sum_c \left(\frac{M_{a,j}}{m_a} - \frac{M_{c,j}}{m_c} \right) m_c w'_{ac} e_{ac}^j, \end{aligned}$$

where we just used the definition (1.63) and sped up the calculation using the previously derived derivatives.

This expression for density allows one to define another formulation of the SPH

$$\frac{d}{dt}\mathbf{x}_a = \frac{\mathbf{M}_a}{m_a}, \quad (1.68a)$$

$$\frac{d}{dt}\mathbf{M}_a = - \sum_b \left(\frac{m_a m_b}{\rho_a^2} p_a + \frac{m_a m_b}{\rho_b^2} p_b \right) w'_{ab} \mathbf{e}_{ab}, \quad (1.68b)$$

$$\frac{d}{dt}\rho_a = \sum_b \left(\frac{\mathbf{M}_a}{m_a} - \frac{\mathbf{M}_b}{m_b} \right) \cdot \mathbf{e}_{ab} w'_{ab} m_b \quad (1.68c)$$

It must be stressed that we do not have any proofs of the Hamiltonianity of the above equations; for them to be Hamiltonian, they must be generated by a Poisson bracket of the state variables $\mathbf{x}_a, \mathbf{M}_a, \rho_a$. Our SPH Poisson bracket (1.60) happens to *not* be the one.

Fortunately, there exists such a Poisson bracket, but we will not provide a derivation of it. The reason is that we preferably aim to use the system (1.67a) instead (for which we have done justice when deriving it), as it is symplectic (for details, see Section 1.4.5), and also the calculation being tedious. In Kincl et al. [2023a], the authors have shown that the Poisson bracket

¹²Note that explicit position dependency is present through the interpolation kernel: $w_{ab} = w(\|\mathbf{x}_a - \mathbf{x}_b\|)$.

$$\begin{aligned} \{F, G\}^{(SPH), \rho} &= \sum_a \left(\frac{\partial F}{\partial x_a^i} \frac{\partial G}{\partial M_{a,i}} - \frac{\partial F}{\partial M_{a,i}} \frac{\partial G}{\partial x_a^i} \right) + \\ &+ \sum_a \sum_b m_b w'_{ab} e^{i_{ab}} \left[\frac{\partial F}{\partial \rho_a} \left(\frac{\partial G}{\partial M_{a,i}} - \frac{\partial G}{\partial M_{b,i}} \right) - \frac{\partial G}{\partial \rho_a} \left(\frac{\partial F}{\partial M_{a,i}} - \frac{\partial F}{\partial M_{b,i}} \right) \right], \end{aligned} \quad (1.69)$$

generate the system of equations (1.65a) above.

At first sight, not even the latter equations seem to be the same as in the scheme (1.51a). Let us try to rewrite them in terms of velocity $\frac{d}{dt} \mathbf{x}_a = \mathbf{u}$:

$$\frac{d}{dt} \mathbf{x}_a = \mathbf{u}_a = \frac{\mathbf{M}_a}{m_a}, \quad (1.70a)$$

$$\frac{d\mathbf{u}_a}{dt} = -\frac{1}{m_a} \sum_b \left(\frac{m_a m_b}{\rho_a^2} p_a + \frac{m_a m_b}{\rho_b^2} p_b \right) w'_{ab} \mathbf{e}_{ab} = -\sum_b m_b \left(\frac{p_a}{\rho_a^2} + \frac{p_b}{\rho_b^2} \right) w'_{ab} \mathbf{e}_{ab}, \quad (1.70b)$$

$$\frac{d\rho_a}{dt} = \sum_b \underbrace{(\mathbf{u}_a - \mathbf{u}_b)}_{\mathbf{u}_{ab}} \cdot \mathbf{e}_{ab} m_b w'_{ab}, \quad (1.70c)$$

which is equivalent to the system (1.51a) ¹³.

We discuss the qualitative differences of equations (1.67a) and (1.68a) in the next section.

Hamiltonian vs symplectic systems

The major difference between the systems (1.67a) and (1.68a) is that the first one is symplectic (and thus Hamiltonian) and the latter one is only Hamiltonian (non-symplectic). Kincl and Pavelka [2023]. We briefly introduce the differences and relationships while keeping the focus on our usage, which is not differential geometry but numerical solutions of ODE's. For details, see any book about differential geometry and symmetries in physics, e.g. Oliva [2002].

A symplectic manifold is a pair (\mathcal{M}, ω) , where \mathcal{M} is a manifold and a ω is a symplectic 2-form on it, that is, a mapping $\omega : \mathcal{M} \times \mathcal{M} \mapsto \mathbb{R}^n$ satisfying

$$d\omega = 0, \quad (1.71a)$$

$$i_{\mathbf{X}} \omega = \omega(\cdot, \mathbf{X}) = 0 \Leftrightarrow \mathbf{X} = \mathbf{0}, \quad (1.71b)$$

$$(1.71c)$$

meaning the form is closed and non-degenerate Oliva [2002]. In classical mechanics, the ‘‘canonical’’ symplectic manifold is the pair $(T^* \mathcal{Q}, d\theta_0)$, where Podolsky [2019]

$$T^* \mathcal{Q} \text{ is the cotangent bundle of the configuration manifold } \mathcal{Q} \quad (1.72a)$$

$$\omega = d\theta_0 = \mathbf{d}p_j \wedge \mathbf{d}q^j \text{ is the outter derivative of the Cartan one-form } \theta_0 = p_j \mathbf{d}q^j \quad (1.72b)$$

¹³With the exception of the absenitng gravity \mathbf{g}_a , which we have not included in our energy functional (1.57)

The cotangent bundle is the "space of momenta p_j ", and the configuration manifold is the "space of positions q^j ". It is convenient to define universal coordinates as $(z^1, z^2, \dots, z^n, z^{n+1}, \dots, z^{2n}) \equiv (q^1, q^2, \dots, q^n, p_1, p_2, \dots, p_n)$. On every symplectic manifold, a *canonical* Poisson bracket is *given using the symplectic 2-form*; given functions f, g of the state variables p_j, q^j , their canonical Poisson bracket always is

$$\{f, g\} = \frac{\partial f}{\partial z^\beta} \omega^{\beta\alpha} \frac{\partial g}{\partial z^\alpha}, \quad (1.73)$$

where $\omega^{\beta\alpha}$ is the inverse symplectic two form expressed in the coordinate basis ¹⁴

$$\omega^{\beta\alpha} = \begin{bmatrix} 0 & -I \\ I & 0 \end{bmatrix}, \quad (1.74)$$

and I stands for the $(n \times n)$ identity matrix. However, there are many physical systems governed by the Hamilton canonical equations, but there does not exist a symplectic 2-form such that (1.73) describes its dynamics - they are governed by a more general Poisson bracket:

$$\frac{d}{dt} z^\beta = \{z^\beta, H\} = L^{\beta\alpha} \frac{\partial H}{\partial z^\alpha}, \quad (1.75)$$

meaning

$$\frac{d}{dt} q^j = \frac{\partial H}{\partial p_j} \quad (1.76)$$

$$\frac{d}{dt} p_j = -\frac{\partial H}{\partial q^j} \quad (1.77)$$

The object $L^{\beta\alpha}$ is the coordinate representation of the Poisson bivector. So far, we have seen there exist various Poisson brackets. *All* of them are generated by some Poisson bivector $L^{\beta\alpha}$, while some are generated by a symplectic 2-form (more precisely, its inverse). This leads us to the following definitions:

A system whose dynamics is described by a Poisson bracket (i.e. by the Hamilton canonical equations induced by it) that is *generated by a symplectic 2-form* ω is referred to as a symplectic system. For symplectic systems, the coordinate representations of the Poisson bivector and the inverse of the symplectic 2-form coincide, $L^{\beta\alpha} \equiv \omega^{\beta\alpha}$

On the other hand, many systems are governed by Hamilton canonical equations induced by a *general* Poisson bracket (such as the rigid body) - an anti-symmetric bivector satisfying the Jacobi identity and the Leibniz rule, and at the same time, *there does not exist a symplectic 2-form generating the bracket* in the fashion of (1.73). These systems are referred to as Hamiltonian systems.

We are interested in symplectic systems mainly because of the ability to deploy symplectic integrators (more generally, structure-preserving integrators) when solving their governing equations. For a particular class of problems, symplectic integrators guarantee an upper bound in total energy error and other valuable qualities Hairer et al. [2004]. An example of such a symplectic integrator is

¹⁴Inverse in the sense that $\omega^{\beta\alpha} \omega_{\gamma\sigma} = \delta_\gamma^\beta \delta_\sigma^\alpha$. The inverse must exist since the form is nondegenerate

the Störmer-Verlet method Hairer et al. [2003]; it has been shown in Kincl and Pavelka [2023] that the symplectic system (1.67a) is globally time reversible when using the Störmer-Verlet method. Therefore, it is preferable to use system (1.67a) instead of system (1.68a) ((1.51a) respectively). On the contrary, the symplectic system’s density treatment creates questionable behavior at the boundaries. This issue, however, was again resolved in Kincl and Pavelka [2023] using fixed-point arithmetic and a correction of the initial conditions.

1.5 Summary of the SPH method

In the previous sections, we have introduced the main results of the SPH method theory. This paragraph aims to summarize them briefly.

The “classical” approach to smoothed particle hydrodynamics starts with the idea of abstract particles, which represent (discretize) a (sub)region of a continuous medium. The governing partial differential equations of the field functions (density, velocity) are rewritten in a simplified form using interpolated (continuously and later discretely) fields and differential operators, yielding a set of ordinary differential equations. Namely, the discretized continuity equation (1.45) and the discretised Euler equations (1.48) should be solved while providing a state equation for the pressure, for example, the expression (1.50).

Another approach to the SPH springs from the consistency of the theory with Hamiltonian mechanics. A very similar system of equations (1.67a) (which agrees well with the particle nature of the method) can be straightforwardly derived from a “discretized” (canonical) Poisson bracket of the continuum mechanics (meaning the equations represent the Hamilton canonical equations generated by the bracket). This origin immediately proves the system’s symplecticity, allowing the use of symplectic integrators. Using a different non-canonical Poisson bracket, another system of ODE’s (1.68a), identical to the “classical” equations of SPH, can be derived, showing consistency with the previous results.

2. Mountain-Wave Simulations in general

2.1 Introduction

The atmosphere is a complex dynamical system. It ranges from the surface of Earth up to about 10 000 km above, is made up of various chemical elements, and exhibits complicated phenomena, such as the weather. An interesting property of the atmosphere is its ability to support the existence of waves of many types, such as the ubiquitous internal gravity waves including orographic generated ones (e.g. lee waves).

It is well known (and will also be discussed in what follows) that the density, pressure, and temperature of air generally change with height. When air ascends to a region of lower density (e.g. upward), the buoyancy force acting on it decreases and is consequently accelerated downwards due to gravity. If the density change is sufficient, on its way back it then overshoots its initial position, reaches a region of higher density, and is again propelled upwards. This oscillatory, “spring-like” motion is a prototype of an internal gravity wave. Sutherland [2010]

Orographic gravity waves can be triggered by flows near the surface. Air traveling along the surface is rapidly lifted upwards when it hits a mountain barrier and because of stratification, buoyancy, and gravity, internal gravity waves can emerge. Orographic gravity waves that are triggered by flow over a mountain barrier (or some other topography) are also called mountain waves. Durran [2003]

2.1.1 Current status of mountain-wave simulations

Why are we interested in mountain waves? Mountain waves play an important role in atmospheric dynamics. They can trigger or amplify downslope windstorms Durran [2003] (extremely strong winds on the slopes of some topographic barriers), generate regions of clear air turbulence (i.e., turbulent flows that lack visual clues such as clouds) and have an impact on dynamics and transport, for example, by mixing of the chemical constituents in the regions of their dissipation. Doyle et al. [2011]. Their multiscale nature prevents the global models from fully representing them. Hence, it is of great interest to be able to accurately simulate mountain waves at least in regional domains.

In the article “An Intercomparison of T-REX Mountain-Wave Simulations and Implications for Mesoscale Predictability” by J. Doyle et al. (Doyle et al. [2011]), flow over mountain terrain has been simulated using 11 different numerical models. The terrain has been modeled using five idealized mountain profiles (given as analytical curves by some function) and one real mountain profile, a section of the Sierra Nevada. All models showed consistency in the baseline experiment with a linear wave theory (parameters of which will be given in later sections). Surprisingly, the results of the other five experiments, where nonlinear effects emerge, vary greatly - in the number and amplitude of the emerging mountain waves, in wind speeds, or in the triggering of downslope windstorms.

Doyle et al. [2011]. The goal of this thesis is to conduct the baseline experiment using the Smoothed Particle Hydrodynamics method, a method mainly used in solid and fluid mechanics.

2.2 An introduction to the theory of internal gravity waves

In this section, we derive a few very basic results of the theory of internal gravity waves, considering the context of this text. For a more thorough description, see, e.g. Nappo [2013] or Sutherland [2010].

We start with the concept of stratification, as it is an essential aspect of the whole theory.

2.2.1 Density and pressure stratification of the atmosphere

Under the assumption that the viscosity of the atmosphere can be neglected, the dynamics of the gas is governed by the Euler equations (the law of conservation of momentum) (1.47)

$$\rho \frac{D\mathbf{u}}{Dt} = -\nabla p + \rho \mathbf{g} - 2\boldsymbol{\Omega} \times \rho \mathbf{u}, \quad (2.1)$$

where we have also included the Coriolis force. Choosing an (inertial) frame of reference and setting $\mathbf{g} = -g\mathbf{e}_z$ while assuming the gas does not accelerate in the vertical axis, the corresponding derivative vanishes and the Euler equation for the vertical direction reads as

$$\frac{dp}{dz} = -\rho g \quad (2.2)$$

This is the hydrostatic balance equation Sutherland [2010]. In fact, it is a (partial) differential equation that connects the vertical pressure gradient to the distribution of the density (recall that the density is a field variable); note particularly that the remaining Euler equations can remain general even with the condition of hydrostatic balance. To solve for pressure and density, one has to specify the equation of state, that is, the relation $p = p(\rho)$. In the formulation of the SPH method (see section 1.3.3) we have introduced the barotropic formula (1.50). However, in our context, it is essential to incorporate the temperature also into our model. Thus, we opt for the thermal equation of the ideal gas:

$$p(T, V, N) = \frac{NRT}{V}, \quad (2.3)$$

where p stands for the pressure, T for the absolute temperature, N for the number of particles (atoms or molecules) of the gas and $R = 8.314 \text{ JK}^{-1} \text{ mol}^{-1}$ is the molar gas constant. With some manipulation, we obtain the following

$$p = \frac{RT}{V} N = \frac{RT}{V} \frac{m}{M_m} = \frac{m}{V} \frac{R}{M_m} T = \rho \bar{R} T, \quad (2.4)$$

where M_m is the molar mass and $\bar{R} = R/M$ is the specific molar gas constant which for dry air equals $\bar{R} = 287,053 \text{ JK}^{-1}\text{kg}^{-1}$. Using this equation, the condition of hydrostatic balance becomes

$$\bar{R} \frac{d(\rho T)}{dz} = -g\rho \quad (2.5)$$

Under the assumption of an isothermal atmosphere we can write

$$\frac{d\rho}{dz} = -\frac{g}{\bar{R}T}\rho, \quad (2.6)$$

and this differential equation has an unique solution

$$\rho(z) = \rho_0 \exp\left(-\frac{g}{\bar{R}T}z\right), \quad (2.7)$$

where $\rho_0 = \rho(z = 0)$. Using the equation (2.4) gives us the pressure dependency

$$p(z) = \bar{R}T\rho_0 \exp\left(-\frac{g}{\bar{R}T}z\right) = p_0 \exp\left(-\frac{g}{\bar{R}T}z\right), \quad (2.8)$$

where naturally $p_0 = p(z = 0) = \bar{R}T\rho_0$. As the altitude increases, both the pressure and density decrease exponentially, but for a fixed altitude, the xy plane forms an isosurface of both the density and pressure. In the case the quantities of state are functions of the vertical coordinate, we say the atmosphere is stratified.

Potential temperature

Briefly, we discuss a general atmospheric state with a non-constant temperature. However, we will only assume adiabatic processes (expansions and compressions). The first law of thermodynamics in molar form for an adiabatic process reads as follows

$$du = \delta W = -p dv, \quad (2.9)$$

using the caloric state equation for an ideal gas $U = c_V RT$, $dU = c_V R dT$ and differentiating the thermal equation $pv = RT$ gives $p dv + v dp = R dT$, so $-p dV = v dp - R dT$. Using these relations, the first law takes the form

$$c_v dT = v dp - R dT \quad (2.10)$$

Next, we deploy the Mayer equation for an ideal gas in the form $c_p - c_v = R$ and use the thermal equation once more to eliminate the volume:

$$c_p dT = \frac{RT}{p} dp, \quad (2.11)$$

rearranging gives the differential equation

$$\frac{dp}{p} = \frac{c_p}{R} \frac{dT}{T} \quad (2.12)$$

Integrating both sides then yields

$$\log \frac{p}{p_0} = \frac{c_p}{R} \log \frac{T}{T_0} = \log \left(\frac{T}{T_0} \right)^{\frac{c_p}{R}} \quad (2.13)$$

Solving for T_0 finally gives

$$\theta := T_0 = T \left(\frac{p_0}{p} \right)^{\frac{R}{c_p}} \quad (2.14)$$

The last relation gives a definition of the potential temperature θ Sutherland [2010]. It is the temperature (dry) air would have when adiabatically moved from pressure p to the pressure p_0 . Potential temperature is especially useful for its conservative nature. It follows from the definition that the potential temperature remains constant under adiabatic flows. We have also obtained the solution for the thermodynamic temperature

$$T = T_0 \left(\frac{p}{p_0} \right)^{\frac{R}{c_p}}, \quad (2.15)$$

and the thermal state equation also gives us the density solution

$$\rho = \frac{p}{RT} = \frac{1}{RT_0} p \left(\frac{p}{p_0} \right)^{\frac{-R}{c_p}} = \frac{p_0}{RT_0} \frac{p}{p_0} \left(\frac{p}{p_0} \right)^{\frac{-R}{c_p}} = \rho_0 \left(\frac{p}{p_0} \right)^{\frac{1}{\gamma}}, \quad (2.16)$$

where we have denoted $\rho_0 = \frac{p_0}{RT_0}$, $\gamma = c_p/c_v$ and used the Mayer equation $c_p - c_v = R$.

2.2.2 Buoyancy oscillations

In the Introduction, we have mentioned the emergence of oscillations in the atmosphere due to the buoyancy force. Using the tools from the previous section, we are now ready to derive the differential equations governing these motions.

Assume a small idealized air parcel with density ρ_p and volume V_p , so that $m_p = \rho_p V_p$ is its mass. Further, assume that the parcel is in a state of thermodynamic equilibrium with its environment, a non-rotating (meaning there is no Coriolis force) atmosphere. The total force acting on the particle consists of the gravity force and the buoyancy force:

$$\mathbf{F} = \mathbf{g}(m_p - m_a), \quad (2.17)$$

where we have used Archimedes principle and denoted m_a to be the mass of the surrounding air displaced by the air particle. Suppose that the particle is displaced from its equilibrium height z_0 by a small perturbation δz - such as the ascending motion caused by hitting a mountain profile. Choosing a frame of reference whose vertical axis is oriented in the opposite direction of gravity and deploying Newton's second law yields

$$m_p \frac{d^2}{dt^2}(\delta z) = -g(m_p - m_a), \quad (2.18)$$

we further assume that the volume of the displaced air V_a is the same as the volume of the particle $V_a = V_p$ and that the pressure relaxes instantaneously

- meaning that the pressure in the air particle is the same as the background pressure. With these assumptions, we can write the following

$$\frac{d^2}{dt^2}(\delta z) = -g \frac{m_p - m_a}{m_p} = -g \frac{\rho_p V_p - \rho_a V_p}{\rho_p V_p} = -g \frac{\rho_p - \rho_a}{\rho_p} = -g \frac{T - T_p}{T}, \quad (2.19)$$

and for the last equality we have used the thermal state equation. If the displacement δz is small enough, the temperature of the air particle T_p and the temperature of the atmosphere T do not differ much from the temperature at height z_0 , denoted T_0 . In other words, we can use the Taylor expansion and drop any terms higher than the linear one

$$ppT_p(z_0 + \delta z) \approx T_0 + \frac{\partial T_p}{\partial z}(z_0)\delta z \quad (2.20)$$

$$T(z_0 + \delta z) \approx T_0 + \frac{\partial T}{\partial z}(z_0)\delta z, \quad (2.21)$$

substituting into the equation above yields

$$\frac{d^2}{dt^2}(\delta z) = -g \frac{T - T_p}{T} = -g \frac{\frac{\partial T}{\partial z} - \frac{\partial T_p}{\partial z}}{T} \delta z \quad (2.22)$$

Since we have supposed the motion of the air particle is adiabatic, we can express its temperature gradient in terms of the adiabatic lapse rate $\Gamma = -\frac{\partial T_p}{\partial z} = \frac{g}{c_p}$ ¹ Nappo [2013] and write

$$\frac{d^2}{dt^2}(\delta z) = -\frac{g}{T} \left(\frac{g}{c_p} - \frac{\partial T}{\partial z} \right) \delta z \quad (2.23)$$

It is convenient to express the former relation using the potential temperature, as it is conserved under adiabatic flows, rather than thermodynamic temperature. Taking the logarithmic derivative of the expression (2.14) reads as

$$\frac{1}{\theta} \frac{\partial \theta}{\partial z} = \frac{1}{T} \frac{\partial T}{\partial z} - \frac{R}{c_p} \frac{1}{p} \frac{\partial p}{\partial z}, \quad (2.24)$$

which under hydrostatic balance and per unit mass reads as (again using the thermal state equation)

$$\frac{1}{\theta} \frac{\partial \theta}{\partial z} = \frac{1}{T} \frac{\partial T}{\partial z} - \frac{1}{T} \frac{g}{c_p} \quad (2.25)$$

Substituting this term into the equation of motion finally gives

$$\frac{d^2}{dt^2}(\delta z) = -\frac{g}{\theta} \frac{\partial \theta}{\partial z} \delta z \quad (2.26)$$

We see that if

$$\frac{\partial \theta}{\partial z} > 0 \quad (2.27)$$

¹As when discussing the potential temperature, the first law of thermodynamics takes the form $c_p dT = \frac{RT}{p} dp$, so per unit volume we have $c_p dT = dp$, invoking hydrostatic balance $dp = -\rho g dz$ yields $c_p dT = -\rho g dz$, from which it is convenient to set $\Gamma = -\frac{dT}{dz} = \frac{g}{c_p}$

the equation (2.26) is the equation of a harmonic oscillator with the “stiffness of the spring” $\frac{\partial\theta}{\partial z}$. The condition that the potential temperature rises with altitude (2.27) is often referred to as the atmosphere is stably stratified Nappo [2013].

In the case of a stably stratified atmosphere, the frequency of the oscillations is given by

$$N = \sqrt{\frac{g}{\theta} \frac{\partial\theta}{\partial z}} \quad (2.28)$$

This frequency is referred to as the Brunt–Väisälä frequency Nappo [2013].

3. Mountain-Wave Simulations using the SPH Method

In the sections 1 and 2 we have introduced Smoothed Particle Hydrodynamics and the theory of mountain waves. The goal of this section is to produce a synthesis of the previous parts - an attempt to simulate mountain waves using the formalism of SPH. Concretely, our aim is to reproduce the baseline experiment posed in Doyle et al. [2011], whose details are discussed in the following.

At this point, it should be noted that SPH has not been used in meteorology before, at least to the best of our knowledge. There exist applications of the SPH method in oceanology to simulate oceanic internal gravity waves. However, ocean salt water has different qualities than air; mainly, it is described by the barotropic state equation (1.50). As it has been discussed in 2.2.1, in the (simplified models) of atmosphere, the density and pressure decrease exponentially, which proves to be a challenge for SPH and its numerical stability; this will be discussed in the section 4.1. With no previous references, we endeavor to utilize the formalism in this rather exotic setting.

The simulations have been conducted using the package `SmoothedParticles.jl` Kincl and Pavelka (Kincl and Pavelka [2023] Kincl et al. [2023c] Kincl et al. [2023b]). The code used to achieve our results is available at `SPH Mountain-Waves` and is also given as an attachment to this text.

3.1 Parameters of the simulation

The authors of Doyle et al. [2011] have set the parameters of their baseline experiment to allow easy reproduction. Here, we present those parameters and discuss their implementation in the formalism of SPH.

3.1.1 Computational domain and mountain profile

The computational domain is a rectangular region, the height of which is 26 km and the length of which is 400 km. Any particles that would leave the domain during the simulation are automatically removed.

A mountain obstacle is placed in the center of the domain. The baseline experiment considers an idealized profile, known as the Witch of Agnesi profile. The elevation of the topography is given by the function

$$h(x) = \frac{h_m a^2}{x^2 + a^2}, \quad (3.1)$$

where h_m is the height of the mountain and a is its “half-width”¹. We take $h_m = 100$ m, $a = 10$ km. The profile is plotted below 3.1

¹In the sense that $h(a) = \frac{h_m}{2}$

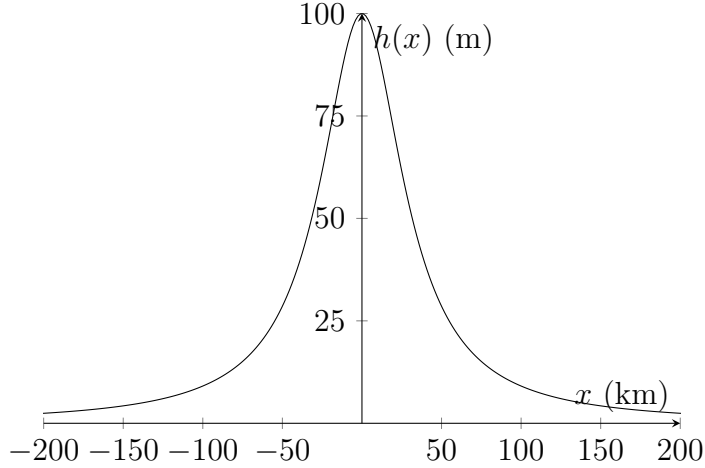


Figure 3.1: The Witch of Agnesi mountain profile

3.1.2 Initial and boundary conditions

Recall that we are solving (a discretized) system of partial differential equations, and thus we have to prescribe some initial and boundary conditions. Setting the initial conditions in the SPH formalism is simple - just prescribe the values of velocity, density, pressure, and temperature at the initial time. However, unlike grid methods, correctly prescribing boundary conditions poses a greater challenge Vacondio et al. [2020]. We cover the conditions one by one.

Initial conditions

To solve the SPH equations, we prescribe initial conditions for the field variables and close the equations by providing an equation of state - the thermal state equation of an ideal gas (2.4). The initial conditions are listed in the table 3.1 below

velocity \mathbf{u}	$\mathbf{u}(0, \mathbf{x}) = U_0 \mathbf{e}_x, U_0 = 20 \text{ m/s}$
pressure p	$p(0, \mathbf{x}) = p_0 \exp\left(-y \frac{g}{RT_0}\right), p_0 = \rho_0 \bar{R} T_0$
density ρ	$\rho(0, \mathbf{x}) = \rho_0 \exp\left(-y \frac{g}{RT_0}\right), \rho_0 = 1.393 \text{ kg/m}^3$
temperature T	$T(0, \mathbf{x}) = T_0, T_0 = 250 \text{ K}$

Table 3.1: Initial conditions for the baseline experiment from the article Doyle et al. [2011]

The initial condition represent an isothermal atmosphere in hydrostatic balance, which has been discussed in 2.2.1. Unfortunately, issues with the stability of the hydrostatic balance (the initial state) have arisen, supposedly due to the massive density differences: $\rho(y = 0) = 1.393 \text{ kg m}^3$ (density of dry air at 250 K and atmospheric pressure) and at the top $\rho(y = 26 \text{ km}) = 0.0398 \text{ kg m}^3$. More discussion of this issue is presented in 4.1.1.

Boundary conditions

The computational domain has 4 boundaries: 2 lateral, top and bottom + mountain. The baseline simulation in Doyle et al. [2011] prescribes the free slip boundary condition at the bottom and open lateral boundaries. The top boundary condition depends on the numerical model; however, the majority uses Rayleigh damping. Let us discuss the implementation of all these boundary conditions.

Lateral conditions *seem* straightforward. In the west ², there is a constant inflow of particles with the initial conditions given by the table 3.1. In the east, the domain is open and all particles that escape it are removed. Realize, however, that this technically means vacuum - the particles pushed from the domain do not feel any resistance from the particle outside the domain as there are none. In other words, there exists a pressure gradient that drives the particles. We discuss this problem in the following section 4.1.3.

The bottom boundary condition is the no-slip condition. In recent years, great progress has been made in field boundary value problems in the SPH formalism Macia et al. [2011]. The simplest way to ensure no slip is to create “dummy” particles outside the domain. Those particles are treated as the standard fluid particles, i.e., they are included in the calculation of the velocities, pressure, etc., but their positions remain constant and their velocities and accelerations are kept as zero. Notice that this rather complicated way of treating boundary conditions is inherent to the SPH method and is a considerable downside of the formalism. Macia et al. [2011]

At the top boundary, Rayleigh damping has been chosen to impose the boundary condition. The Rayleigh damping technique consists of creating a layer from height y_b to height y_t , in which the v velocity component (i.e., the vertical component, $\mathbf{u} = (u, v)$) is damped Durran and Klemp [1983]. The structure of the damping layer is determined by the function introduced in Durran and Klemp [1983]

$$\gamma(y) = \begin{cases} \gamma_r \sin^2 \left(\frac{\pi}{2} \left(1 - \frac{y_t - y_b}{y_b} \right) \right), & \text{for } y \in [y_b, y_t] \\ 0, & \text{elsewhere} \end{cases} \quad (3.2)$$

The value γ_r is the strength of the damping, the typical values being $\gamma_r \approx 10N$ (a guide on how to find an appropriate value can be found in Klemp and Lilly [1978]), where $N^2 = 0.0196 \text{ s}^{-1}$ is the Brunt–Väisälä frequency, which we take the same as the authors of Doyle et al. [2011]. ³

Our implementation of Rayleigh damping consists of subtracting the term (3.2) at each integration time step. Note that in e.g. Klemp and Lilly [1978] the numerical method used for the simulation was the finite difference method (i.e., a grid method) and that SPH requires principally a different approach. It should be determined by experiment whether our implementation is suitable or not. Ideally, no other top boundary condition needs to be prescribed; also, no

²“In the west” and “in the east” just means “on the left side” and “on the right side”, but said by a meteorologist.

³It can be shown that for a dry isothermal atmosphere the B-V frequency is $N^2 = \frac{g^2}{C_p T_0}$ Nappo [2013], so by setting the same temperature T_0 in our simulation, we are certain to obtain the same (at least analytically) B-V frequency.

solid boundary is needed at the top, as free surface is natural to the atmosphere⁴. However, due to the instability of the hydrostatic balance, a solid boundary had to be introduced at the top of the domain; see section 4.1.1.

⁴Notice that modeling free surfaces in the SPH method is very simple.

4. Results of the simulation

The last chapter deals with the results of the simulations. In truth, it deals primarily with the problems encountered in obtaining the results and then attempts to determine a course of action for the future. The topic turned out to be much more complex, and some of the challenges could not be solved with the given resources.

4.1 Challenges

Alltogether, total of four different simulations have been carried out to simulate the emergence of mountain waves.

1. A static isothermal state of the atmosphere without any inflow or outflow
2. A flow over a mountain range within an isothermal atmosphere
3. A static state of the atmosphere without any inflow or outflow, supposing all (potential ¹) processes are adiabatic
4. An adiabatic flow over the mountain range

The simulations grow in complexity from 1. to 4. Basically, when assuming the atmosphere remains isothermal throughout the whole evolution (cases 1.,2.), the simple set of equations (1.65a) together with the thermal state equation of an ideal gas (2.4) is sufficient. Clearly, this is a primitive attempt to simulate physical reality, and there is little hope to simulate a phenomenon such as an internal gravity wave. In the more general cases 3. and 4., when the temperature evolves only with adiabatic constraints, a more thermodynamically rich description is required. The easiest approach to calculate the temperature of a SPH particle in the SPH formalism is by introducing entropy as a state variable. The theory has been developed, for example, in Kincl et al. [2023a].²The temperature of an ideal gas expressed in terms of variables appropriate for the SPH method can be written as:

$$T = \frac{\rho^{\gamma-1}}{c_V(\gamma-1)} \exp\left(\frac{s}{c_V\rho}\right), \quad (4.1)$$

where ρ is the (mass) density, $\gamma = \frac{c_P}{c_V}$ is the Poisson constant, c_V is the specific heat capacity at a constant volume and s is the entropy density. For more details, see the article Kincl et al. [2023a].

However, serious issues even with the idealized simulations 1. and 2. have been faced. We discuss them in the following sections.

¹Ideally, the atmosphere should be completely static.

²As we have discussed in the introduction to section 1.4, due to the required deeper knowledge of continuum thermodynamics, we do not provide a derivation of the governing equations of the “entropic SPH”.

4.1.1 Hydrostatic balance

The baseline experiment in Doyle et al. [2011] suggests that the *initial state* of the ambient atmosphere is isothermal and in hydrostatic balance (2.2). Naturally, the first simulation that has been conducted is exactly the simulation of this special state. Ideally, air should not exhibit any motion throughout the simulation and also all field variables, such as the pressure, density, or potential temperature should remain constant.

That was not the case. In the beginning of the simulation, a spurious wave began to propagate upward, resulting in total loss of stability of the initial condition; see figure 4.1.

Similarly, a simulation of a hydrostatic balance with the adiabatic constraints has been run with qualitatively the same results; see figure 4.2.

To stabilize the hydrostatic balance, three different precautions were made:

1. Replace the free surface at the top of the domain with a solid wall
2. Deploy a packing algorithm
3. Dissipate the spurious energy of the initial state by introducing extreme viscosity

We discuss these attempts in the upcoming sections.

Top boundary condition

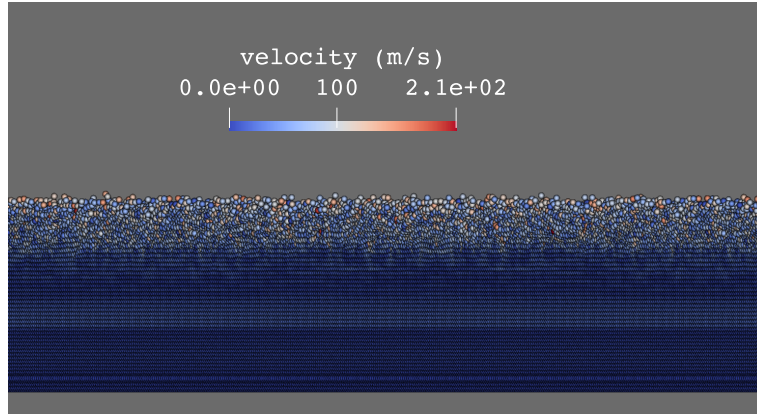
Originally, free surface was prescribed at the top boundary (together with the Rayleigh damping). This showed to be impractical. As can be seen from the figures 4.1 and 4.2, due to the vertically propagating wave and the absence of a solid boundary, a large amount of gas was rapidly ejected upwards. When the gas dropped back to the surface, the impact caused the whole atmosphere to totally lose its stability. So, a solid boundary was added at the top together with a no slip boundary condition ³

The introduction of the top boundary wall was helpful in eliminating the instability caused by the impact of the gas, however, did not (and possibly could not from the beginning) resolve the issue with the propagating wave.

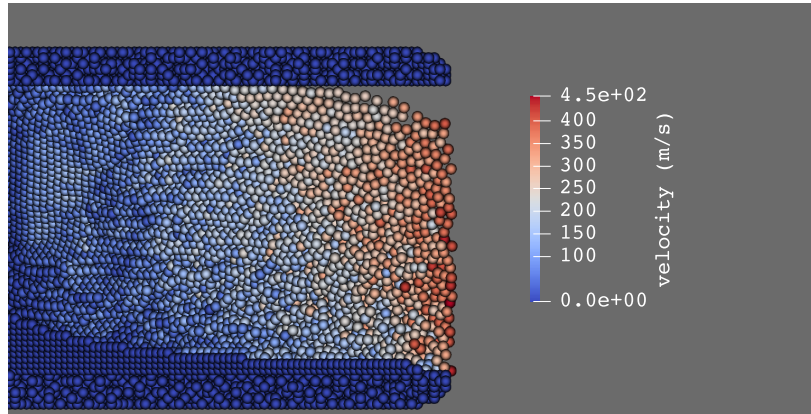
Packing algorithm

It has been discussed many times in the SPH literature, that the stability of the initial condition remains as an unpleasant numerical artifact of the method Violeau [2012] Monaghan [2005]. A simple and robust way to deal with this issue has been presented in the article Colagrossi et al. [2012]. It consists of a preprocessing procedure, that is run before the actual simulation starts. Simply said, one of the causes of the instability is the unregularity of the initial particle distribution. The procedure in a clever way minimizes this “unevenness” of the distribution. For details, see the article Colagrossi et al. [2012].

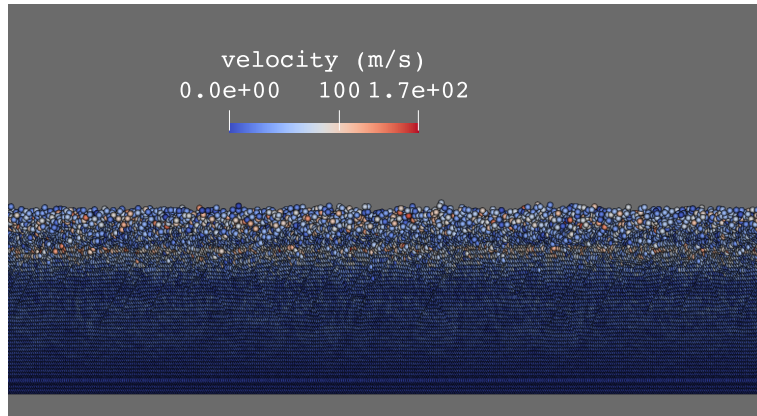
³A free slip condition would seem more natural here, as we only aim to eliminate the normal component of velocity. Truth is, no slip is easier to implement in the SPH method and there showed to be no difference between the two conditions whatsoever.



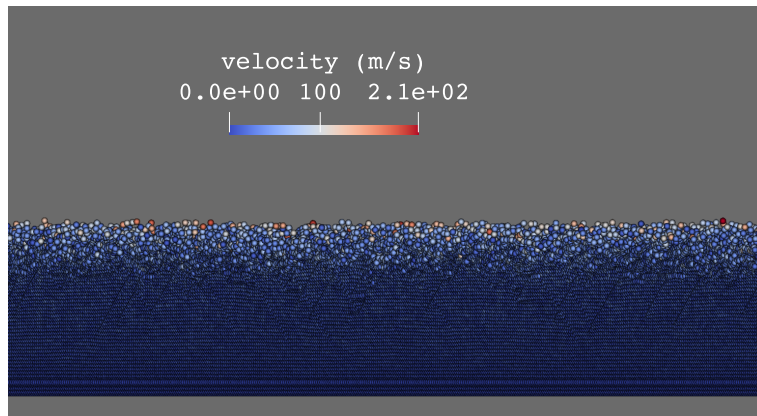
(a) The magnitude of velocity at t=50 s



(b) The magnitude of velocity at t=100 s

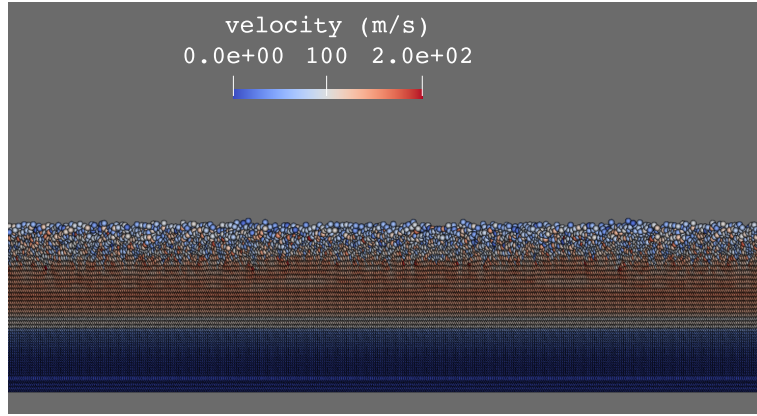


(c) The magnitude of velocity at t=150 s

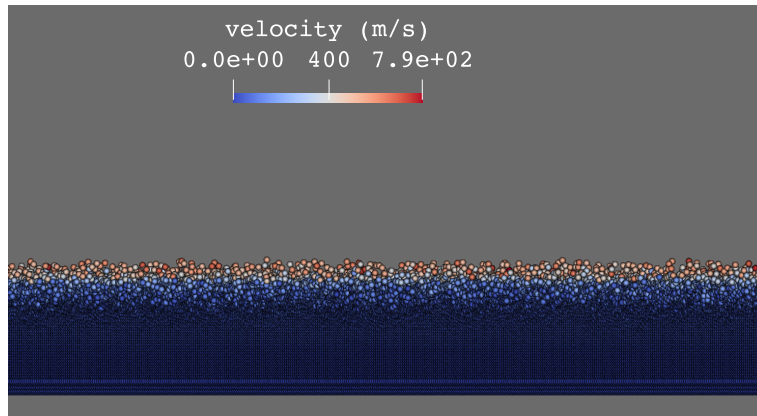


(d) The magnitude of velocity at t=200 s

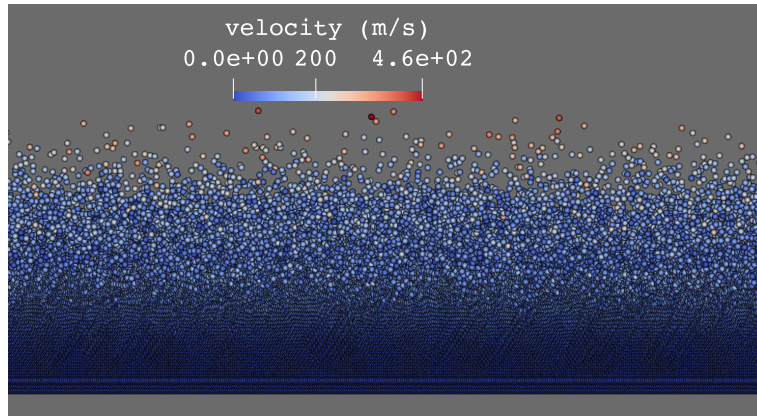
Figure 4.1: The magnitude of velocity in a isothermal static atmospheric state, central part of the domain



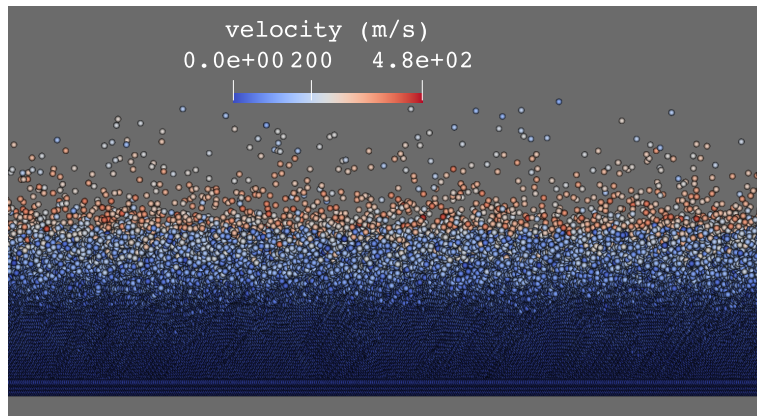
(a) The magnitude of velocity at t=50 s



(b) The magnitude of velocity at t=100 s



(c) The magnitude of velocity at t=150 s



(d) The magnitude of velocity at t=200 s

Figure 4.2: The magnitude of velocity in an adiabatic static atmospheric state, central part of the domain

The packing algorithm has been implemented and can be found in the attached files. Experiments with it showed, that after the packing procedure, the particles seemed to be aligned in a hexagonal grid (at first, a square grid to initialize them has been used). Observing this, in the later simulations, the particles have been initialized in a hexagonal grid.

The hexagonal alignment showed to be somewhat helpful in stabilizing the hydrostatic balance, although it only *reduced* the effect of the propagating wave; it did not eliminate it completely.

Stabilization through dissipation

The final attempt to stabilize the initial condition was inspired by the procedure introduced by J. Monaghan Monaghan [2005]. The simulation is initialized with a very high dynamic viscosity (e.g., $\nu = 1.0$ Pa s, whereas the dynamical viscosity of dry air at 250 K is $\nu = 16 \cdot 10^{-6}$ Pa s). This leads to massive dissipation of energy that the initial state possesses and should result in a state with lower energy that is hopefully more stable. This state is then used as an initial state of the actual simulation.

With all the precautions combined, the first and third simulations from the list 4.1 (the static cases) have been conducted again; this time, to better capture long-time stability, the model simulated 4 hours of evolution. The results for the adiabatic simulation after each hour are shown in the figure 4.3.

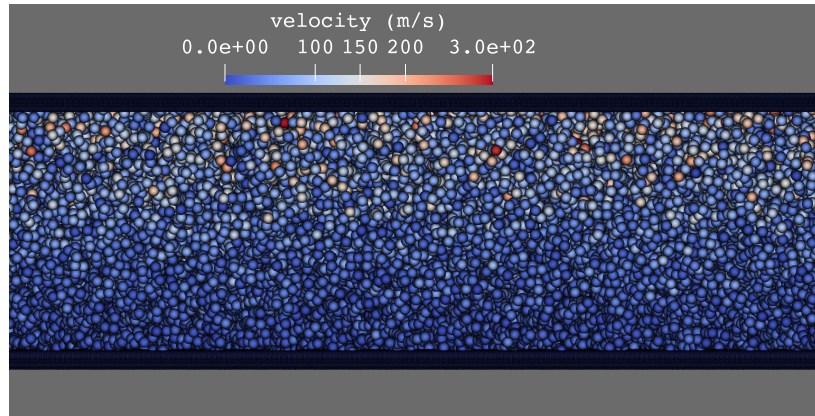
4.1.2 Further procedure after unsatisfactory attempts to stabilize the hydrostatic balance

It is clear that only after the first hour of the simulation, the hydrostatic balance is far from static. At this point, it became evident that simulating the 4 h evolution of a flow (as those are the parameters of the baseline experiments from Doyle et al. [2011]) would prove impossible. Internal gravity waves are subtle buoyancy oscillations and our model showed significant oscillations even when none should be present.

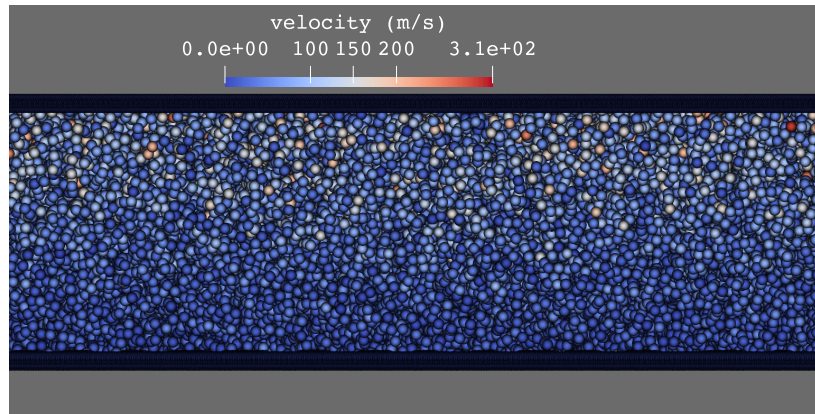
At that moment a decision was made as to how to proceed when pursuing the goal of the thesis. Instead of trying to simulate internal gravity waves and compare our results to the experiments conducted in Doyle et al. [2011], due to the reasons above, it has been chosen to rather invest our resources into developing the methodology of the SPH method in meteorology, without strictly using the same setting as in Doyle et al. [2011]. That is why we in the upcoming sections use different parameters of the simulation - mainly the dimensions of the computational domain and the parameters of the Witch of Agnesi profile (3.1).

4.1.3 Boundary conditions

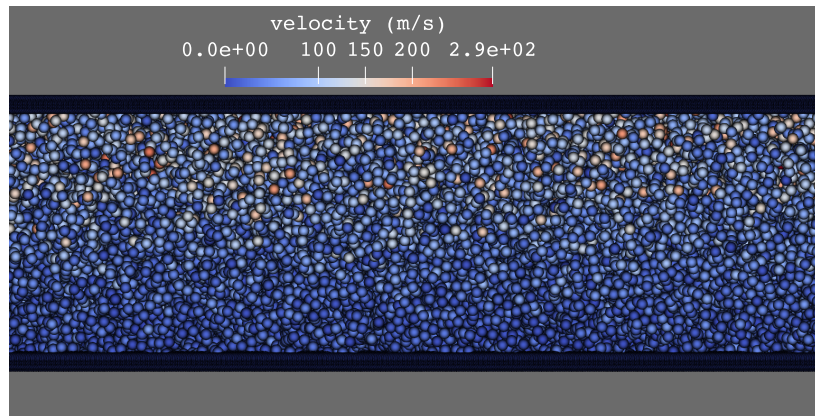
Treating boundary conditions is considered as a great challenge in the SPH formalism Vacondio et al. [2020]. We faced a challenge in implementing an open boundary condition at the east part of the domain, i.e., at the outflow.



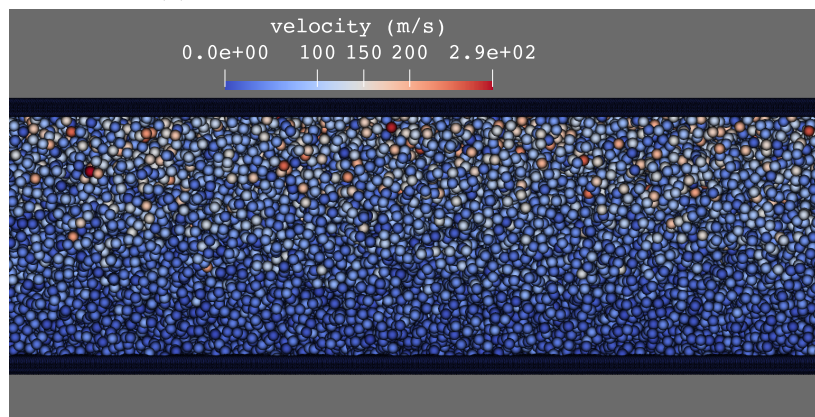
(a) The magnitude of velocity at $t = 1$ h



(b) The magnitude of velocity at $t = 2$ h



(c) The magnitude of velocity at $t = 3$ h



(d) The magnitude of velocity at $t = 4$ h

Figure 4.3: The magnitude of velocity in a diab. atmo. state after improvements, central part of the domain

Outflow

The naive attempt to only remove the boundary wall particles at the east side of the domain and let the outflowing particles simply vanish ⁴ proved unsuitable. As obviously no particles are present outside of the domain, the particles close to the boundary do not feel any resistance when leaving the domain. Technically, this means that the outflow is into vacuum and a tumultuous decompression occurs. This effect is visible in the figure 4.4

To fix this phenomenon, a different arrangement of the computational domain has been designed; it is depicted in the figure 4.5. The outflow region is at the top boundary wall so that the gravity force acting on the leaving particles slows them and prevents the decompression. But mainly, the pressure at the top part of the domain has been subtracted from the pressure of each individual particle, resulting in zero pressure at the outflow. Using this modification, there is no pressure gradient at the interface. The simulations have been conducted again with these modifications, the results can be seen in the figure 4.6 and the state of the whole atmosphere can be seen in the figure 4.7.

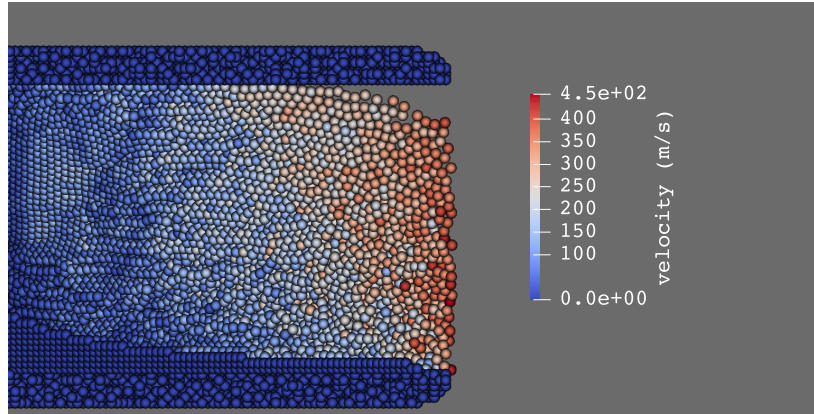
The attempts showed to have no significant improvement. What is more, as it is evident from the figure 4.7, the modification resulted in vacancies in the particle distribution throughout the whole computational domain.

4.1.4 Sound waves

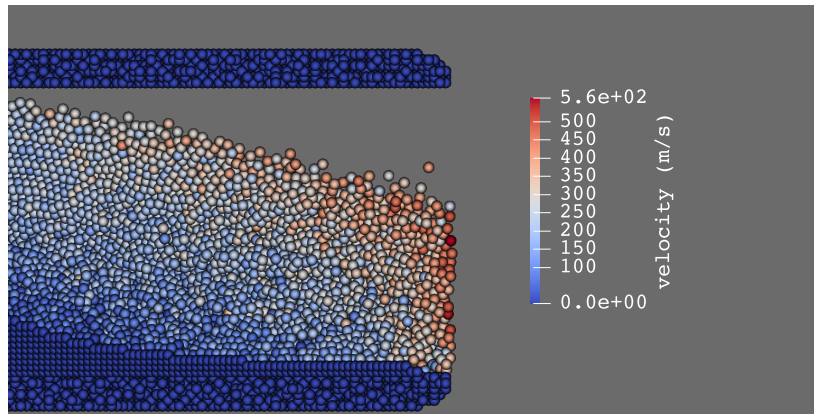
In the presentation above, we have come across important stability issues when trying to simulate the atmospheric dynamic using the Euler equations and a simple ideal gas thermal state equation. The choice of the Euler equations is standard in the WCSPH scheme (weakly compressible smoothed particle hydrodynamics) Violeau [2012]. In this work, we have also chose the WCSPH scheme, as it is rather simple and no previous attempts known to the author to simulate the atmosphere using any SPH formalism have been made. However, it is not customary in simulating internal gravity waves in meteorology to use the unmodified version of the Euler equations. One of the reason being that the Euler equations capture also the dynamics of sound waves, not only internal gravity waves. Sound waves typically possess much faster dynamics than internal gravity waves and as such they mean a threat to the stability of numerical models. Sutherland [2010]. To account for the instabilities caused by sound waves, meteorologists use a variety of techniques, such as the anelastic approximation. By assuming certain facts about the variations of the background density and pressure, it can be shown that a different set of equations that does not support the emergence of sound waves can be derived; for details, see Sutherland [2010] or Nappo [2013].

It is not clear what effects on stability do sound waves have in our simulations. However, implementing the anelastic approximation in the SPH formulation should be considered in further attempts to use the SPH method in meteorology.

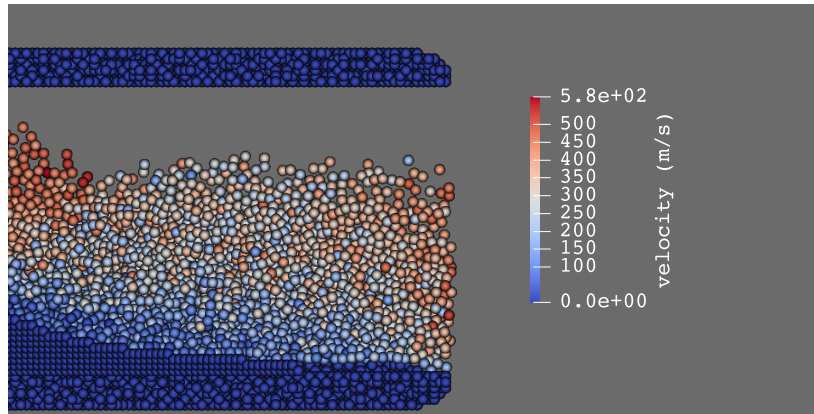
⁴The `SmoothedParticles.jl` package we used to run the simulations automatically removes all the particles that exit the computational domain.



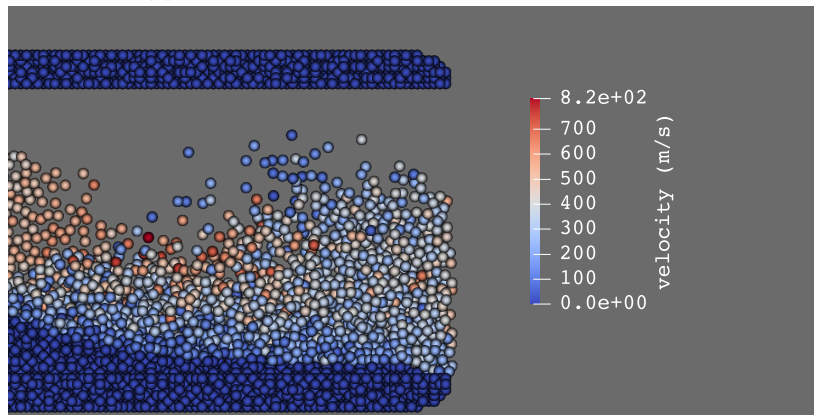
(a) The magnitude of velocity at $t = 100$ s



(b) The magnitude of velocity at $t = 200$ s



(c) The magnitude of velocity at $t = 300$ s



(d) The magnitude of velocity at $t = 400$ s

Figure 4.4: The rapid decompression at the outflow due to vacuum outside the domain

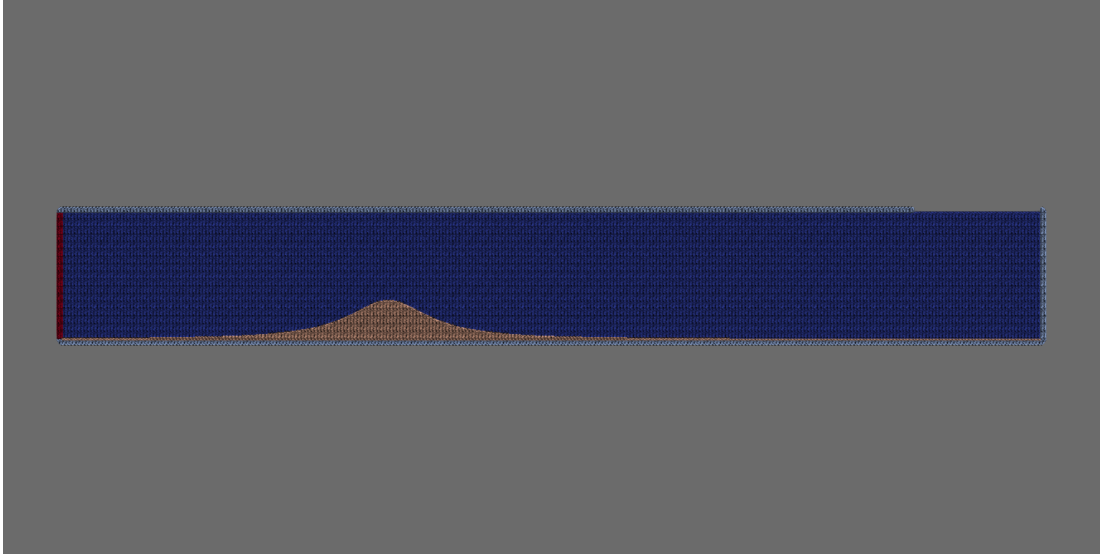
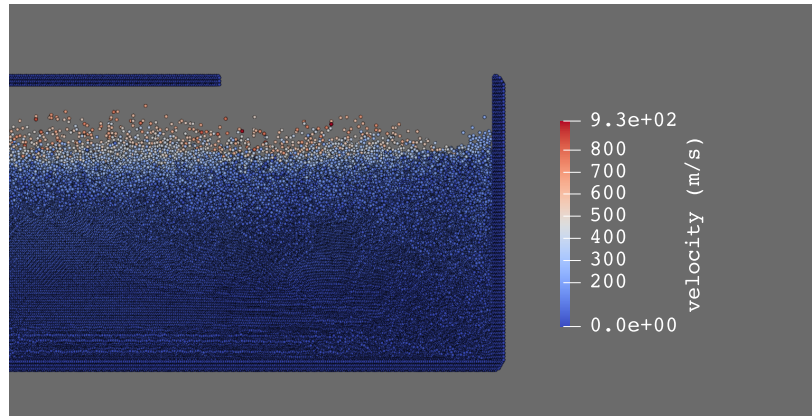


Figure 4.5: The computational domain adopted to counter the decompression effect

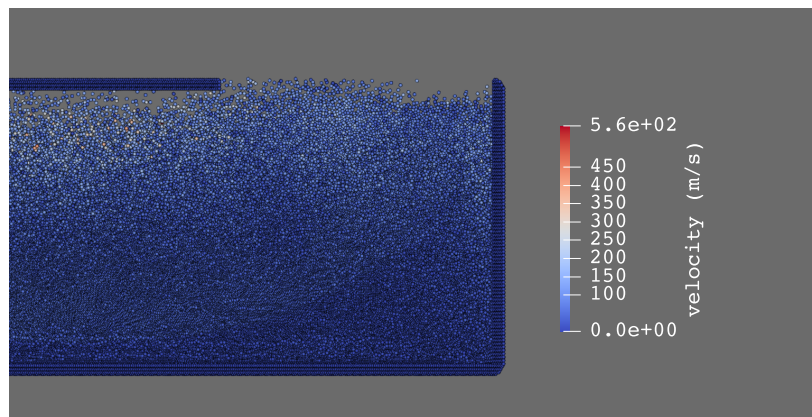
4.2 Results

In this last section, we show some results from the simulation experiments. The code (a mildly modified version of it) used to obtain these results can be found in the attached files to this text. As the issues addressed in previous sections could not be resolved, the relevance of the results presented here is disputable. It must be noted that the attempt to recreate the baseline experiment from Doyle et al. [2011] and to capture mountain waves cannot be successful under the current condition of the used model.

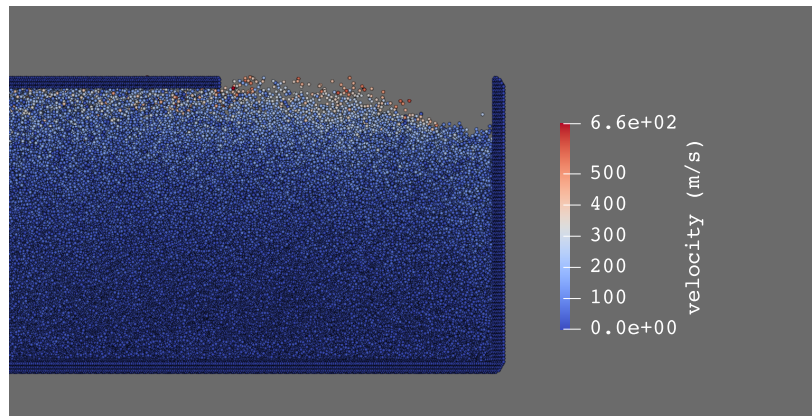
As in the many times discussed article, we evaluate the profile of potential temperature and the vertical component of velocity. We only do so for the adiabatic flow (case 4. from 4.1), as the previous 3 cases were just simplified versions of the simulation. The results can be found in the figures 4.8 and 4.9. The vertical velocity component seems to be distributed chaotically with respect to both orientation and magnitude. The potential temperature remains somewhat static in the lower parts of the domain and is influenced heavily by the vacancies at the top part of the domain.



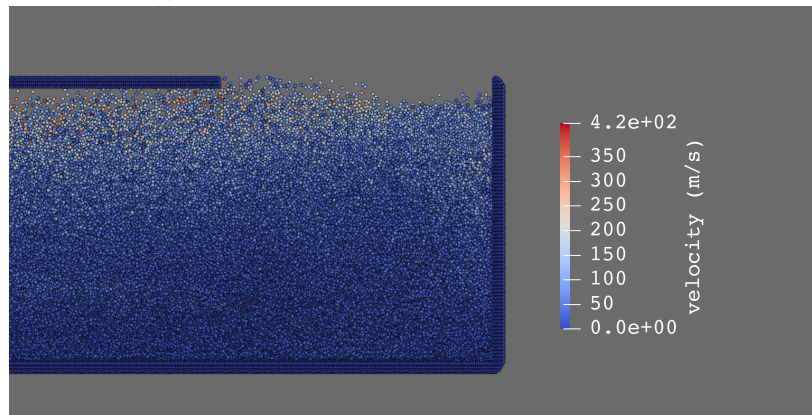
(a) The magnitude of velocity at $t = 100$ s



(b) The magnitude of velocity at $t = 200$ s



(c) The magnitude of velocity at $t = 300$ s



(d) The magnitude of velocity at $t = 400$ s

Figure 4.6: An attempt to fix the rapid decompression at the outflow due to vacuum outside the domain

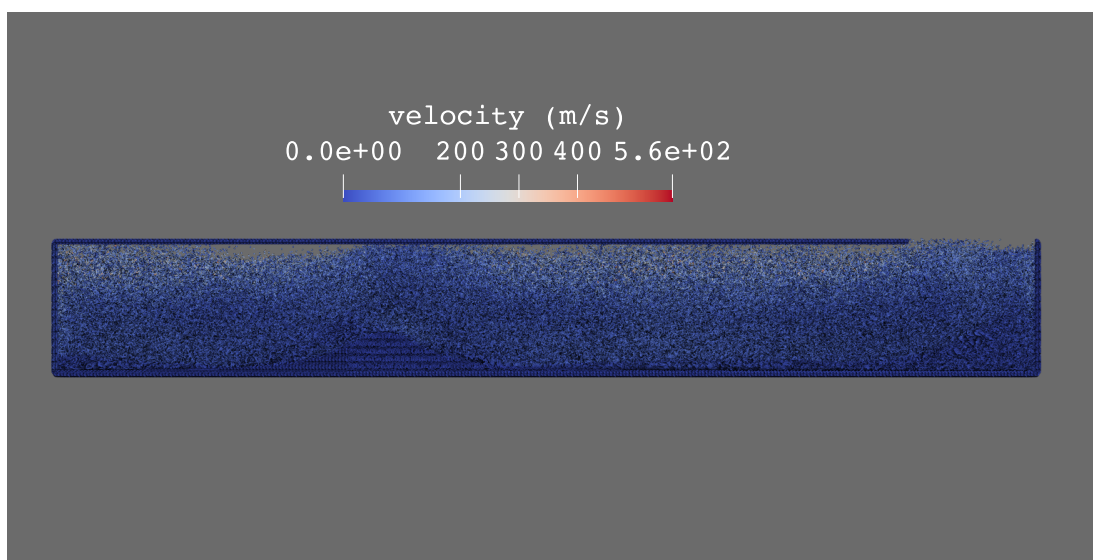
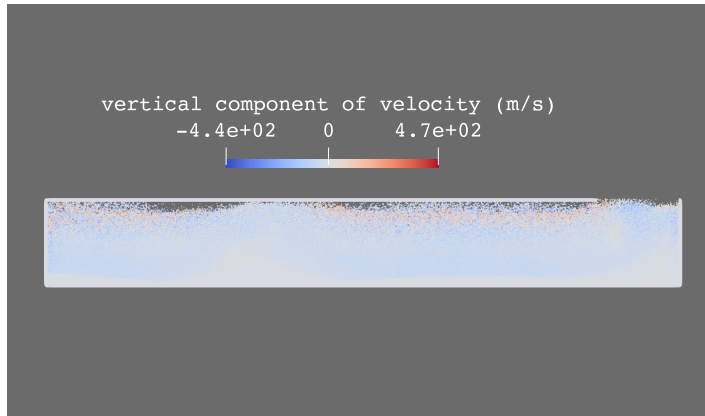
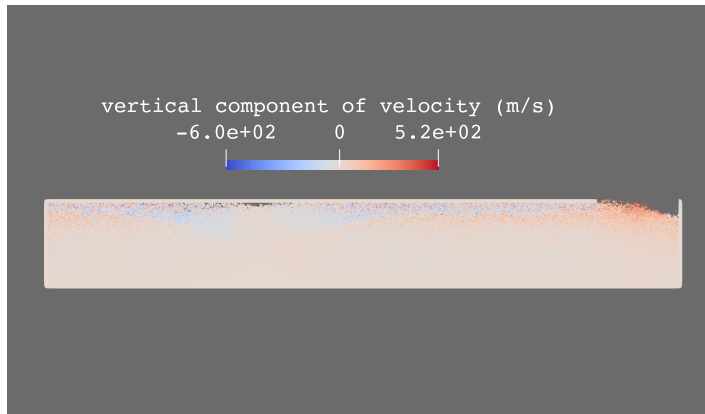


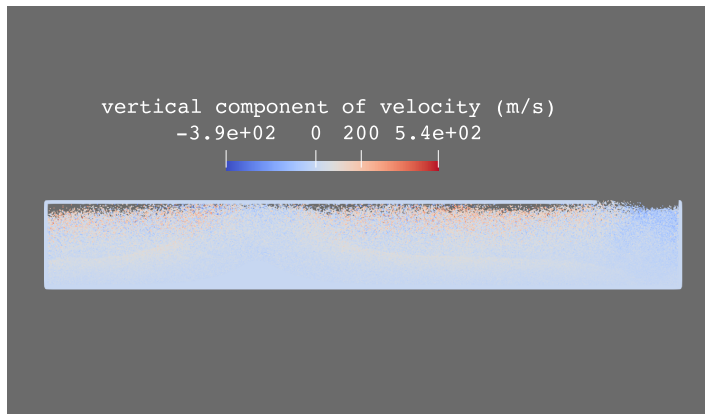
Figure 4.7: The vacancies in the domain due to the decompression at the outflow



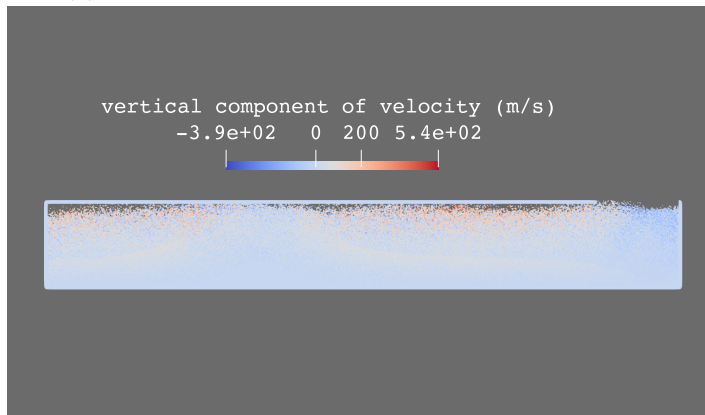
(a) The vertical velocity component at $t = 1$ h



(b) The vertical velocity component at $t = 2$ h

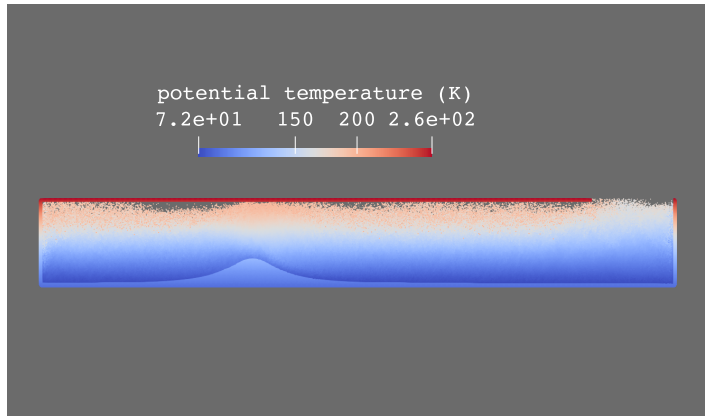


(c) The vertical velocity component at $t = 3$ h

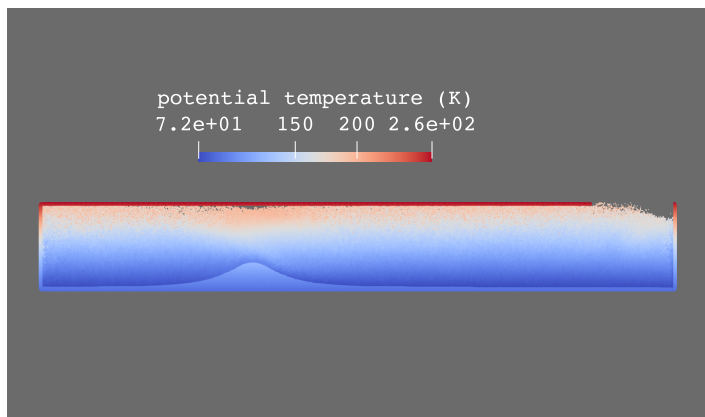


(d) The vertical velocity component at $t = 4$ h

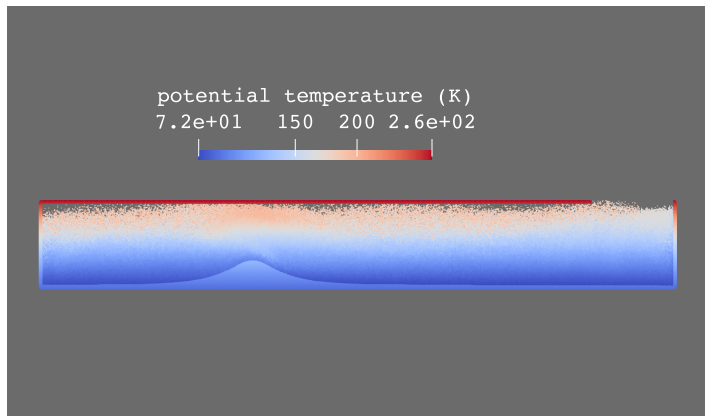
Figure 4.8: The vertical component of velocity at different times



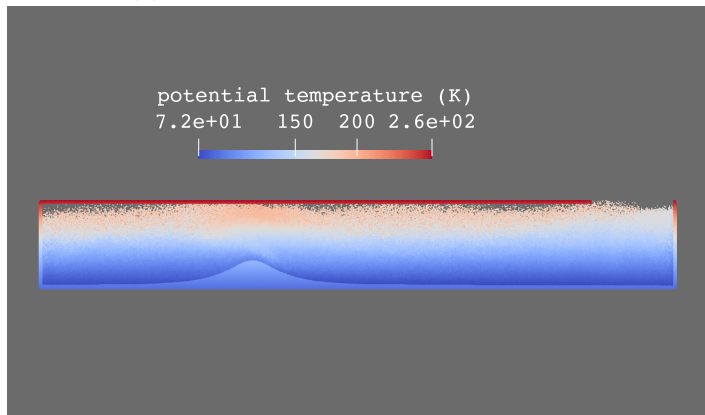
(a) Potential temperature at t = 1 h



(b) Potential temperature at t = 2 h



(c) Potential temperature at t = 3 h



(d) Potential temperature at t = 4 h

Figure 4.9: The profile of the potential temperature at different times

Conclusion

There are four goals of this thesis

- provide an introduction to the SPH method (chapter 1)
- briefly summarize mountain-wave simulations (chapter 2)
- address some aspects of those simulations in the SPH formalism (chapter 3)
- conduct numerical experiments (chapter 4)

When working on the first goal, we have introduced the key points of the SPH method: particle discretization of the domain, continuous and discrete interpolation of field functions and later differential operators. These approaches were used to discretize the continuity equation and the Euler equations; together with an equation of state, these relations are the foundation of the (weakly compressible) smoothed particle hydrodynamics.

We have mentioned that one of the benefits of the SPH method is its consistency with the formalism of Hamiltonian mechanics. Following this approach, we have come again to the same (and also some others) formulation of the governing equations, but this time with the proof of their symplecticity/Hamiltonianity. Because of this, we were allowed to deploy the symplectic Störmer-Verlet integration scheme when solving the governing equations.

In the second chapter, we have provided the foundations of the theory of internal gravity waves and mountain waves. Of essential importance showed to be the concept of stratification, which on the other hand later proved to be the biggest challenge in our numerical simulations. We have introduced the Brunt–Väisälä frequency of the oscillations, a function of the potential temperature governing the frequency of the oscillations (at least in the linearized case). Potential temperature, being a versatile variable in meteorology, has been evaluated later in our simulations.

The third chapter discusses the implementation of the setting of our numerical experiment in the SPH formalism. It deals mainly with initial and boundary conditions, which are generally uneasy to implement in the SPH formalism. For example, we had to come up with an implementation of the top boundary condition.

With all of the ingredients, we have made a great effort to capture the emergence of mountain waves in our numerical experiments. Consequently, we have faced problems with the model: the instability of the hydrostatic balance and the decompression at the outflow. To stabilize the hydrostatic balance, we have implemented a packing algorithm, a pre-processing procedure that tries to improve the initial particle distribution. We have combined this algorithm with an attempt to stabilize the initial state by introducing a very large dissipation (viscosity) with the intention of lowering the energy of the initial state. Both of our attempts proved to be inadequate and the hydrostatic balance could not be stabilized. We have also faced an issue when implementing the open boundary condition. Initially, as we have simply removed the solid wall, an artificial vacuum

was essentially created. That resulted in rapid decompression. To solve this, we changed the geometry of the domain and made the outflow region in the top boundary and also subtracted a constant pressure term, hoping that gravity and the absence of a pressure gradient would solve our decompression problem. It did not.

Finally, with all the flaws still being present, we have run a 4 hour simulation of an adiabatic atmospheric flow over a mountain obstacle on a computer cluster. Unfortunately, we were unable to simulate any internal gravity waves.

The task of simulating such a subtle phenomenon as an orographic gravity wave, without any existing references or software, proved to be much more difficult than expected. Before trying to run a complex simulation, more work needs to be done to stabilize the hydrostatic balance, and a more sophisticated treatment of the outflow needs to be deployed. The author of this text hopes that the work presented in the thesis might be of use as a starting point to future development of the SPH formalism in the context of orographic gravity waves.

Bibliography

- Andrea Colagrossi, B. Bouscasse, M. Antuono, and S. Marrone. Particle packing algorithm for sph schemes. *Computer Physics Communications*, 183(8):1641–1653, August 2012. ISSN 0010-4655. doi: 10.1016/j.cpc.2012.02.032.
- James D. Doyle, Saša Gaberšek, Qingfang Jiang, Ligia Bernardet, John M. Brown, Andreas Dörnbrack, Elmar Filaus, Vanda Grubišić, Daniel J. Kirshbaum, Oswald Knoth, Steven Koch, Juerg Schmidli, Ivana Stiperski, Simon Vosper, and Shiyuan Zhong. An intercomparison of t-rex mountain-wave simulations and implications for mesoscale predictability. *Monthly Weather Review*, 139(9):2811–2831, September 2011. ISSN 1520-0493. doi: <https://doi.org/10.1175/MWR-D-10-05042.1>.
- Dale R. Durran and Joseph B. Klemp. A compressible model for the simulation of moist mountain waves. *Monthly Weather Review*, 111(12):2341–2361, December 1983. ISSN 1520-0493. doi: [https://doi.org/10.1175/1520-0493\(1983\)111<2341:ACMFTS>2.0.CO;2](https://doi.org/10.1175/1520-0493(1983)111<2341:ACMFTS>2.0.CO;2).
- D.R. Durran. Lee waves and mountain waves. pages 1161–1169, 2003. doi: 10.1016/B0-12-227090-8/00202-5.
- R. A. Gingold and J. J. Monaghan. Smoothed particle hydrodynamics: theory and application to non-spherical stars. *Monthly Notices of the Royal Astronomical Society*, 181(3):375–389, December 1977. ISSN 1365-2966. doi: <https://doi.org/10.1093/mnras/181.3.375>.
- M. E. Gurtin and W. J. Drugan. *An Introduction to Continuum Mechanics*, volume 51. ASME International, December 1984. doi: <https://doi.org/10.1115/1.3167763>.
- E. Hairer, C. Lubich, and G. Wanner. Geometric numerical integration: Structure preserving algorithms for ordinary differential equations, 2004.
- Ernst Hairer, Christian Lubich, and Gerhard Wanner. Geometric numerical integration illustrated by the störmer–verlet method. *Acta Numerica*, 12:399–450, May 2003. ISSN 1474-0508. doi: <https://doi.org/10.1017/S0962492902000144>.
- Ondrej Kincl and Michal Pavelka. Globally time-reversible fluid simulations with smoothed particle hydrodynamics. *Comput. Phys. Commun.*, 284:108593, 2023. doi: 10.1016/J.CPC.2022.108593.
- Ondrej Kincl, Michal Pavelka, and Vaclav Klika. Approaches to conservative smoothed particle hydrodynamics with entropy. Unpublished manuscript, 2023a.
- Ondřej Kincl and Michal Pavelka. SmoothedParticles.jl.
- Ondřej Kincl, Ilya Peshkov, Michal Pavelka, and Václav Klika. Unified description of fluids and solids in smoothed particle hydrodynamics. *Applied Mathematics and Computation*, 439:127579, February 2023b. ISSN 0096-3003. doi: <https://doi.org/10.1016/j.amc.2022.127579>.

- Ondřej Kincl, David Schmoranz, and Michal Pavelka. Simulation of superfluid fountain effect using smoothed particle hydrodynamics. *Physics of Fluids*, 35(4), April 2023c. ISSN 1089-7666. doi: 10.1063/5.0145864.
- J. B. Klemp and D. K. Lilly. Numerical simulation of hydrostatic mountain waves. *Journal of the Atmospheric Sciences*, 35(1):78–107, January 1978. ISSN 1520-0469. doi: [https://doi.org/10.1175/1520-0469\(1978\)035<0078:NSOHMW>2.0.CO;2](https://doi.org/10.1175/1520-0469(1978)035<0078:NSOHMW>2.0.CO;2).
- G. R. (Gui-Rong) Liu. *Smoothed particle hydrodynamics a meshfree particle method* /. World Scientific,, Singapore ; London :, reprinted edition, 2009. ISBN 981-238-456-1. Literaturverz.: 423 - 444.
- F. Macia, M. Antuono, L. M. Gonzalez, and A. Colagrossi. Theoretical analysis of the no-slip boundary condition enforcement in sph methods. *Progress of Theoretical Physics*, 125(6):1091–1121, June 2011. ISSN 1347-4081. doi: <https://doi.org/10.1143/PTP.125.1091>.
- J J Monaghan. Smoothed particle hydrodynamics. *Reports on Progress in Physics*, 68(8):1703–1759, July 2005. ISSN 1361-6633. doi: 10.1088/0034-4885/68/8/R01.
- J.J Monaghan. Extrapolating b splines for interpolation. *Journal of Computational Physics*, 60(2):253–262, September 1985. ISSN 0021-9991. doi: [https://doi.org/10.1016/0021-9991\(85\)90006-3](https://doi.org/10.1016/0021-9991(85)90006-3).
- F. D. Murnaghan. The compressibility of media under extreme pressures. *Proceedings of the National Academy of Sciences*, 30(9):244–247, September 1944. ISSN 1091-6490. doi: <https://doi.org/10.1073/pnas.30.9.244>.
- C. J. Nappo. *An introduction to atmospheric gravity waves*. Number v. Volume 102 in Issn Ser. Elsevier, Waltham, Mass., 2nd ed. edition, 2013. ISBN 9780123852243. Includes bibliographical references and index.
- Waldyr Muniz Oliva. *Geometric Mechanics*. Number v.1798 in Lecture Notes in Mathematics Ser. Springer Berlin / Heidelberg, Berlin, Heidelberg, 2002. ISBN 978-3540442424. Description based on publisher supplied metadata and other sources.
- Michal Pavelka, Václav Klika, and Miroslav Grmela. Multiscale thermodynamics: Introduction to generic. August 2018. doi: <http://dx.doi.org/10.1515/9783110350951>.
- Michal Pavelka, Ilya Peshkov, and Václav Klika. On hamiltonian continuum mechanics. *Physica D: Nonlinear Phenomena*, 408:132510, July 2020. ISSN 0167-2789. doi: <https://doi.org/10.1016/j.physd.2020.132510>.
- Jiri Podolsky. Teoretická mechanika v jazyce diferencální geometrie. Unpublished manuscript, 2019.
- Bruce R. Sutherland. *Internal Gravity Waves*. Cambridge University Press, September 2010. ISBN 9780511780318. doi: <https://doi.org/10.1017/CBO9780511780318>.

Renato Vacondio, Corrado Altomare, Matthieu De Leffe, Xiangyu Hu, David Le Touzé, Steven Lind, Jean-Christophe Marongiu, Salvatore Marrone, Benedict D. Rogers, and Antonio Souto-Iglesias. Grand challenges for smoothed particle hydrodynamics numerical schemes. *Computational Particle Mechanics*, 8(3):575–588, September 2020. ISSN 2196-4386. doi: <https://doi.org/10.1007/s40571-020-00354-1>.

G. L. Vaughan, T. R. Healy, K. R. Bryan, A. D. Sneyd, and R. M. Gorman. Completeness, conservation and error in sph for fluids. *International Journal for Numerical Methods in Fluids*, 56(1):37–62, June 2007. ISSN 1097-0363. doi: [10.1002/fld.1530](https://doi.org/10.1002/fld.1530).

Damien Violeau. *Fluid Mechanics and the SPH Method*. Oxford University Press, May 2012. ISBN 9780199655526. doi: <https://doi.org/10.1093/acprof:oso/9780199655526.001.0001>.